Plant Physiology Preview. Published on October 15, 2014, as DOI:10.1104/pp.114.247494

Corresponding author: Kolby Jardine, Climate Science Department, Earth Science Division, Lawrence Berkeley National Laboratory, One Cyclotron Rd, building 64-241, Berkeley, CA 94720, USA, phone (+55-92-9145-5279), email (kjjardine@lbl.gov)

Research Area: Biochemistry and Metabolism

Dynamic balancing of isoprene carbon sources reflects photosynthetic and photorespiratory responses to temperature stress

[*1]Kolby Jardine, [1]Jeffrey Chambers, [2]Eliane G. Alves, [2]Andrea Teixeira, [2]Sabrina Garcia, [1]Jennifer Holm, [2]Niro Higuchi, [2]Antonio Manzi, [3]Leif Abrell, [4]Jose D. Fuentes, [5]Lars K. Nielsen, [1]Margaret Torn, and [5]Claudia E. Vickers

[1]Corresponding author: Climate Science Department, Earth Science Division, Lawrence Berkeley National Laboratory, One Cyclotron Rd, building 64-241, Berkeley, CA 94720, USA, email (kjjardine@lbl.gov)

[2]National Institute for Amazon Research (INPA), Ave. Andre Araujo 2936, Campus II, Building LBA, Manaus, AM 69.080-97, Brazil

[3]Department of Chemistry & Biochemistry and Department of Soil, Water and Environmental Science, University of Arizona, Tucson, AZ, USA

[4]Department of Meteorology, College of Earth and Mineral Sciences, Pennsylvania State University, University Park, PA, USA

[5]Australian Institute for Bioengineering and Nanotechnology, The University of Queensland, Building 75, Cnr Cooper and College Rds, St. Lucia, QLD, 4072, Australia

Summary: [13]C-labeling studies suggest the uncoupling between photosynthesis and isoprene emissions with temperature reflects the differential temperature sensitivities of photosynthesis and photorespiration.

Footnotes

This research was supported by the Office of Biological and Environmental Research of the U.S. Department of Energy under Contract No. DE-AC02-05CH11231 as part of their Terrestrial Ecosystem Science Program and the National Science Foundation CHE0216226.

Address correspondence to kjjardine@lbl.gov

Abstract

The volatile gas isoprene is emitted in Tg/annum quantities from the terrestrial biosphere and exerts a large effect on atmospheric chemistry. Isoprene is made primarily from recently-fixed photosynthate; however, "alternate" carbon sources play an important role, particularly when photosynthate is limiting. We examined the relative contribution of these alternate carbon sources under changes in light and temperature, the two environmental conditions that have the strongest influence over isoprene emission. Using a novel real-time analytical approach that allowed us to examine dynamic changes in carbon sources, we observed that relative contributions do not change as a function of light intensity. We found that the classical uncoupling of isoprene emission from net photosynthesis at elevated leaf temperatures is associated with an increased contribution of "alternate" carbon. We also observed a rapid compensatory response where "alternate" carbon sources compensated for transient decreases in recently-fixed carbon during thermal ramping, thereby maintaining overall increases in isoprene production rates at high temperatures. Photorespiration is known to contribute to the decline in net photosynthesis at high leaf temperatures. A reduction in the temperature at which the contribution of alternate carbon sources increased was observed under photorespiratory conditions, while photosynthetic conditions increased this temperature. Feeding [2-^{13}C]glycine (a photorespiratory intermediate) stimulated emissions of [$^{13}C_{1-5}$]isoprene and $^{13}CO_2$, supporting the possibility that photorespiration can provide an alternate source of carbon for isoprene synthesis. Our observations have important implications for establishing improved mechanistic predictions of isoprene emissions and primary carbon metabolism, particularly under the predicted increases in future global temperatures.

***Keyword index*: isoprene carbon sources, MEP pathway, photosynthesis, photorespiration, leaf temperature, light, $^{13}CO_2$, [2-^{13}C]glycine**

1. Introduction

Many plant species emit isoprene (2-methyl-1,3-butadiene, C_5H_8) into the atmosphere at high rates (Rasmussen, 1972). With an estimated emission rate of 500-750 Tg per year by terrestrial ecosystems (Guenther et al., 2006), isoprene exerts a strong control over the oxidizing capacity of the atmosphere. Due to its high reactivity to oxidants, it fuels an array of atmospheric chemical and physical processes affecting air quality and climate including the production of ground-level ozone in environments with elevated concentrations of nitrogen oxides (Atkinson and Arey, 2003; Pacifico et al., 2009) and the formation/growth of organic aerosols (Nguyen et al., 2011). At the plant level, isoprene provides protection from stress, through stabilizing membrane processes (Sharkey and Singsaas, 1995; Velikova et al., 2011) and/or reducing the accumulation of damaging reactive oxygen species in plant tissues under stress (Loreto et al., 2001; Vickers et al., 2009b; Velikova et al., 2012). While the mechanism(s) are still under investigation, isoprene may directly or indirectly stabilize hydrophobic interactions in membranes (Singsaas et al., 1997), minimize lipid peroxidation (Loreto and Velikova, 2001), and directly react with reactive oxygen species (Kameel et al., 2014), yielding first order oxidation products methyl vinyl ketone and methacrolein (Jardine et al., 2012b; Jardine et al., 2013). The two main environmental drivers for global changes in isoprene fluxes are light and temperature (Guenther et al., 2006). Isoprene production is closely linked to net photosynthesis, and both isoprene emissions and net photosynthesis are controlled by light intensity (Monson and Fall, 1989). There is also a positive correlation between net photosynthesis and isoprene emissions as leaf temperatures increase up to the optimum temperature for net photosynthesis (Monson et al., 1992).

Despite the close correlation between photosynthesis and isoprene emissions, plant enclosure observations and leaf-level analyses have both shown that the fraction of net photosynthesis dedicated to isoprene emissions is not constant. During stress events that decrease net photosynthetic rates, isoprene emissions are often less affected or even stimulated; this results in an increase in relative isoprene production from 1-2% of net photosynthesis under normal conditions to 15-50% under extreme stress (Goldstein et al., 1998; Fuentes et al., 1999; Kesselmeier et al., 2002; Harley et al., 2004). In severe stress conditions such as drought, isoprene emissions can even continue in the complete absence of photosynthesis (Fortunati et al., 2008). An uncoupling of isoprene emissions from net photosynthesis has also been observed in a number of other studies where the optimum temperature for isoprene emissions was found to be substantially higher than that of net photosynthesis; under the high temperature conditions, isoprene emissions can account for more than 50% of net photosynthesis (Sharkey and Loreto, 1993; Lerdau and Keller, 1997; Harley et al., 2004; Magel et al., 2006).

Analyses of carbon sources using $^{13}CO_2$ leaf labeling have revealed that under standard conditions (i.e., leaf temperature of 30 °C and photosynthetically active radiation (PAR) levels of 1000 µmoles m^{-2} s^{-1}), isoprene is produced primarily (70-90%) using carbon directly derived from the Calvin cycle (Delwiche and Sharkey, 1993; Affek and Yakir, 2002; Karl et al., 2002a) *via* the chloroplastic methylerythritol phosphate (MEP) isoprenoid pathway (Zeidler et al., 1997). The relative contributions of photosynthetic and "alternate" carbon sources for isoprene are now recognized as being variable under different environmental conditions. Changes in net photosynthesis rates under drought stress (Funk et al., 2004; Brilli et al., 2007), salt stress (Loreto and Delfine, 2000), and changes in ambient O_2 and CO_2 concentrations (Jones and Rasmussen, 1975; Karl et al., 2002b; Trowbridge et al., 2012) alter their relative contributions. Under heat stress-induced photosynthetic limitation in *Populus deltoides* (a temperate species), an increase in the relative contribution of alternate carbon sources was also observed (Funk et al., 2004). However, our current understanding of the responses of isoprene carbon sources to changes in temperature and light levels is poor, and the connection(s) of these responses to changes in leaf primary carbon metabolism (e.g. photosynthesis, photorespiration, and respiration) remains to be determined.

Studies over the last decade have shown or suggested that potential alternate carbon sources include refixation of respired CO_2 (Loreto et al., 2004), intermediates from the cytosolic mevalonate isoprenoid pathway (Flügge and Gao, 2005b; Lichtenthaler, 2010), and intermediates from central carbon metabolism, including pyruvate (Jardine et al., 2010), phosphoenolpyruvate (Rosenstiel et al., 2003), and glucose (Schnitzler et al., 2004). Over 40 years ago it was also proposed that photorespiratory carbon could directly contribute to isoprene production in plants (Jones and Rasmussen, 1975); however, subsequent studies (Monson and Fall, 1989; Hewitt et al., 1990; Karl et al., 2002b) have concluded that photorespiration does not contribute to isoprenoid production.

In this study we examined the carbon composition of isoprene emitted from tropical tree species under changes in light and temperature, the two key environmental variables that affect isoprene emissions. Using a novel real-time analytical approach, we were able to observe compensatory changes in carbon source contribution to isoprene during thermal ramping at high temperatures, despite the overall isoprene emissions remaining relatively stable. By conducting leaf temperature curves under variable $^{13}CO_2$ concentrations and applying [2-^{13}C]glycine leaf labeling, we also reopen the discussion on the role of photorespiration as an alternate source of carbon for isoprenoid formation.

2. Results

2.1. Light intensity correlates positively with net photosynthesis and isoprene emissions in mango leaves

Net photosynthesis measurements were made simultaneously with isoprene emission measurements from mango leaves over 0-2000 μmol m^{-2} s^{-1} photosynthetic active radiation (PAR) at a constant leaf temperature of 30 °C. A strong positive correlation between average isoprene emission rates and net photosynthesis rates was observed as these values increased with light intensity (**Figure 1a**; $R^2 = 0.94$), with an average of 3.1 ± 0.3% of carbon assimilated by net photosynthesis emitted in the form of isoprene over the PAR flux range. This demonstrates the classical tight connection between photosynthesis and isoprene emission under these conditions (Monson and Fall, 1989; Loreto and Sharkey, 1990; Harley et al., 1996). As also observed in these previous studies, at light intensities above 500 μmol m^{-2} s^{-1} PAR, a decrease in the quantum yields of both net photosynthesis and isoprene emissions occurred as net photosynthesis rates transitioned from light limiting to carboxylation limiting.

2.2. Variations in light intensity increase photosynthetic carbon sources for isoprene in mango leaves

To gain additional insight into the connections between net photosynthesis, isoprene emissions, and isoprene carbon sources, PAR curves on mango leaves were conducted under $^{13}CO_2$. Incorporation of the ^{13}C-label into isoprene was followed through real-time measurements of isoprene isotopologue emission rates with 0-5 ^{13}C atoms using proton transfer reaction - mass spectrometry (PTR-MS) together with gas chromatography – mass spectrometry (GC-MS) ^{13}C-labeling analysis of isoprene fragment and parent ions C_2, C_4, and C_5. To initiate the experiment, individual mango leaves on plants inside the growth chamber were installed in a darkened leaf cuvette exposed to $^{13}CO_2$. Unlabeled isoprene was released at low levels for 20-30 min, the first 15 min of which was in a darkened cuvette and the remainder of which was at 25 μmol m^{-2} s^{-1} PAR (representative leaf shown in **Figure 1b,c**). Over the remainder of the experiment, [^{12}C]isoprene emissions remained low with relative emissions representing < 5% of total isoprene emissions above 500 μmol m^{-2} s^{-1} PAR.

During the lowest light intensity (25 μmol m^{-2} s^{-1} PAR), overall isoprene emissions were low, and significant ^{13}C-labeled isoprene emissions were not detected. However, above the light compensation point for net photosynthesis (20-40 μmol m^{-2} s^{-1} PAR), emissions of all ^{13}C-labeled isoprene isotopologues were observed. This can also be seen in the GC-MS labeling analysis of isoprene parent and fragment ions (**Figure S1**). [^{12}C]isoprene was gradually replaced with ^{13}C-labeled isoprene, with

[$^{13}C_5$]isoprene dominating by 76-95 min after the experiment started (100 μmol m^{-2} s^{-1} PAR; dark blue curves in **Figure 1b,c**). Relative emissions of [$^{13}C_{1-4}$]isoprene sequentially peaked and then declined. Thus, for PAR fluxes of 0-500 μmol m^{-2} s^{-1}, the relative abundances of [^{12}C]isoprene and [$^{13}C_{1-4}$]isoprene represented a significant fraction of total emissions, although ^{13}C-labeling of isoprene is most likely a function of both PAR intensity and time after re-illumination (**Figure 1b,c**).

From 500-1000 μmol m^{-2} s^{-1} PAR, a strong increase in the absolute emissions of [$^{13}C_5$]isoprene occurred (from 6 to 16 nmol m^{-2} s^{-1}) while unlabeled and partially labeled [$^{13}C_{1-4}$]isoprene emissions remained essentially constant. Thus, despite the persistence of [$^{13}C_{1-4}$]isoprene at high light intensities, the increase in isoprene emissions is entirely due to recently-assimilated $^{13}CO_2$. This results in a strong increase in the relative emissions of [$^{13}C_5$]isoprene and a decrease in relative emissions of [^{12}C]isoprene and [$^{13}C_{1-4}$]isoprene (**Figure 1c**). Above 1000 μmol m^{-2} s^{-1} PAR, emissions of [$^{13}C_5$]isoprene essentially saturate although small increases in emissions rates occurred up to 2000 μmol m^{-2} s^{-1}. This resulted in a stabilization of the relative emissions of [$^{13}C_5$]isoprene up to 72% of total emissions with the remainder comprised of [^{12}C]isoprene (0.1% of total), [$^{13}C_1$]isoprene (1.5% of total), [$^{13}C_2$]isoprene (2.3% of total), [$^{13}C_3$]isoprene (9.0% of total), and [$^{13}C_4$]isoprene (15.1% of total). Thus, essentially all isoprene emissions at 2000 μmol m^{-2} s^{-1} PAR contained at least one ^{13}C atom with a large fraction (72%) completely ^{13}C-labeled ([$^{13}C_5$]isoprene). Consistent with the PTR-MS measurements of relative [$^{13}C_5$]isoprene emissions, the GC-MS data revealed that the increase in isoprene emission ratio R_5 ($^{13}C_5/^{12}C_5$) is largely driven by increases in [$^{13}C_5$]isoprene emissions; [^{12}C]isoprene emissions remained very low and variable at all light levels (Supplementary **Figure S1**).

2.3. Photosynthesis and isoprene emissions show classical temperature responses in mango leaves

Net photosynthesis measurements were made simultaneously with isoprene emission measurements from mango leaves under variations in leaf temperature at constant PAR of 1000 μmol m^{-2} s^{-1} and 400 ppm CO_2. Both net photosynthesis and isoprene emissions increased together as leaf temperature increased from 25.0 - 32.5 °C (**Figure 2a**). Net photosynthesis rates peaked at leaf temperatures between 30.0 - 32.5 °C. Further increases in leaf temperature (32.5 - 42.0 °C) resulted in a strong decline in net photosynthesis rates, whereas isoprene emissions continued to increase, peaking between 37.5 - 40 °C. These results are consistent with previous studies that also revealed different temperature optima for net photosynthesis (~30 °C) and isoprene emissions (~40 °C) (Laothawornkitkul et al., 2009). At temperatures above the optimum for isoprene emission, a decline in emission was observed followed by an increase again in some leaves (**Figure 2a**). When average isoprene emission rates were regressed against those of net photosynthesis rates over the leaf temperature interval of 25.0 - 32.5 °C, a positive correlation was

observed (r^2 = 0.79) with 8.4 ± 3.1% of net photosynthesis being released as isoprene emissions. In contrast, over the leaf temperature interval of 32.5 - 42.0 °C (where isoprene emissions increased but net photosynthesis rates decreased), a negative correlation was observed (r^2 = 0.71). When control temperature curve experiments on mango leaves over the same leaf temperature range were conducted, but in the dark, isoprene emissions remained very low. Significant stimulation of isoprene emissions could not be detected even at the highest leaf temperatures (data not shown).

2.4. Increases in leaf temperature drive compensatory responses in isoprene carbon sources in mango

In order to further investigate isoprene carbon sources in response to temperature changes, leaf temperature curves were made on leaves exposed to $^{13}CO_2$. Upon placing the mango leaf in the chamber at 25.0 °C with 1000 μmol m^{-2} s^{-1} PAR, the leaf continued to release [^{12}C]isoprene for 20-30 minutes (black curves in **Figure 2b,c**). Following this initial release, [^{12}C]isoprene emissions represented less than 4% of total emissions up to leaf temperatures of 32.5 °C. Within 5 min of the leaf being exposed to $^{13}CO_2$ in the light, emissions of all ^{13}C-labeled isoprene isotopologues could be detected. Thus, although the leaf continued to release [^{12}C]isoprene for 20-30 min following exposure to $^{13}CO_2$, ^{13}C-labeled isoprene could already be detected within 5 min. These observations likely reflect the replacement of the ^{12}C-substrates by ^{13}C-labeled precursors derived from photosynthesis. After 5 min, [$^{13}C_5$]isoprene increased sharply, dominating emissions within 11 min and stabilizing at 44% of the total emissions within 20 min (dark blue curves in **Figure 2b,c**). Increasing the leaf temperature to 27.5 °C resulted in enhanced emission rates of [$^{13}C_{3\text{-}5}$]isoprene without significant increases in [$^{13}C_{1\text{-}2}$]isoprene emissions. This resulted in an increase in [$^{13}C_5$]isoprene relative emissions to values up to 55% of the total. While further increases in leaf temperatures from 27.5 °C to 32.5 °C resulted in strong increases in [$^{13}C_5$]isoprene emissions, its contribution to total emissions only slightly increased with a maximum value of 59% at 32.5 °C.

At leaf temperatures above the optimum for net photosynthesis (30.0 - 32.5 °C), an overall trend of declining relative emissions of [$^{13}C_5$]isoprene with increasing leaf temperature was observed; this decrease was compensated for by increases in relative contributions of [^{12}C]isoprene and [$^{13}C_{1\text{-}3}$]isoprene to maintain high isoprene emissions. At leaf temperatures above 32.5°C, enhanced emission dynamics of all ^{13}C-labeled isoprene isotopologues occurred, including periods of rapid depletion of [$^{13}C_5$]isoprene followed by partial recovery (most clearly shown in **Figure 2c**, vertical arrows).

We also analyzed ^{13}C-labeling patterns of GC-MS fragment and parent ions during the temperature curves under $^{13}CO_2$. $^{13}C/^{12}C$ isoprene emission ratios (R) of C_2 ($^{13}C_2/^{12}C_2$, R_2 = m/z 29/27) and C_4 ($^{13}C_4/^{12}C_4$, R_4 = m/z 57/53) fragment ions and C_5 ($^{13}C_5/^{12}C_5$, R_5 = m/z 73/68) parent ions were calculated as a function of

leaf temperature. Consistent with the PTR-MS studies of relative [$^{13}C_5$]isoprene emissions, the peak in R_2, R_4, and R_5 (**Figure 3a**) occurred at the same temperature as the optimum temperature for net photosynthesis (32.5 °C) (**Figure 3b**). Also consistent with the PTR-MS observations of absolute [$^{13}C_5$]isoprene emissions, GC-MS analysis revealed that the absolute emissions of [$^{13}C_5$]isoprene peaked at substantially higher temperatures than net photosynthesis (37.5 - 40.0 °C) whereas [^{12}C]isoprene emissions remained low up to 32.5 °C followed by an increase with temperature (**Figure 3c**).

2.5. Temperature and $^{13}CO_2$ responses in shimbillo

To extend the temperature study to a second tropical species and to examine responses under enhanced and suppressed photorespiratory conditions, temperature response curves were conducted on *Inga edulis* (shimbillo) leaves under different $^{13}CO_2$ atmospheres (low: 150 ppm, medium: 300 ppm, and high: 800 ppm, **Figure 4**). At standard conditions (30 °C leaf temperature and 1000 µmol m^{-2} s^{-1} PAR), total isoprene emissions were much higher under the medium $^{13}CO_2$ concentrations (total isoprene emissions: 80 nmol m^{-2} s^{-1}) than low (total isoprene emissions: 17 nmol m^{-2} s^{-1}) and high $^{13}CO_2$ concentrations (total isoprene emissions: 35 nmol m^{-2} s^{-1}). These results are consistent with what has been previously reported where isoprene emissions show a peak around 300 ppm CO_2 and decline at lower and higher concentrations (Affek and Yakir, 2002). However, this pattern was broken at leaf temperatures above 40 °C where total isoprene emissions under high $^{13}CO_2$ concentrations were similar to those under medium $^{13}CO_2$ concentrations.

Similar to the overall response of the mango leaves at 400 ppm, under the low (150 ppm) and medium (300 ppm) $^{13}CO_2$ concentrations, absolute [$^{13}C_5$]isoprene emissions were stimulated by leaf temperature increases but then declined at higher leaf temperatures (**Figure 4a,b**). As with the mango leaves, this decline in [$^{13}C_5$]isoprene emissions was accompanied by an increase in unlabeled and partially labeled isoprene emissions. This resulted in a clear optimum leaf temperature where the relative [$^{13}C_5$]isoprene emissions (% total) were maximized. Relative to medium $^{13}CO_2$ concentrations, photorespiratory conditions (low $^{13}CO_2$) resulted in a reduction in the leaf temperature at which [$^{13}C_5$]isoprene emissions peaked (% total). Under medium $^{13}CO_2$ concentrations, [$^{13}C_5$]isoprene emissions reached at maximum of 78.2 % at a leaf temperature of 30.0 °C. Under low $^{13}CO_2$ concentrations, [$^{13}C_5$]isoprene emissions reached at maximum of 37.6 % at a leaf temperature of 27.5 °C. In contrast to the low and medium $^{13}CO_2$ conditions, under the high (800 ppm) $^{13}CO_2$ concentrations, absolute [$^{13}C_5$]isoprene emissions continued to increase up to the highest leaf temperature without a detectable decline, paralleling overall isoprene emissions (**Figure 4c**). Moreover, photosynthetic conditions under high $^{13}CO_2$ concentrations resulted in a strong increase in the optimal temperature of [$^{13}C_5$]isoprene emissions (max 68.5 % at 42.0 °C). Thus, the

optimal temperature for relative [$^{13}C_5$]isoprene emissions increased with $^{13}CO_2$ concentrations (150 ppm $^{13}CO_2$: 27.5 °C, 300 ppm $^{13}CO_2$: 30.0 °C, 800 ppm $^{13}CO_2$: 42.0 °C).

2.6. Glycine, a photorespiratory intermediate, is an alternative carbon source for isoprene

In order to examine photorespiration as a carbon source for isoprene, labeling studies were conducted with [2-^{13}C]glycine fed to detached shimbillo branches through the transpiration stream under constant light and temperature conditions while simultaneous ^{13}C-labeling analysis of CO_2 (using cavity ring-down spectroscopy, CRDS) and isoprene (using PTR-MS and GC-MS) was implemented. Emissions of $^{13}CO_2$ were detected within five minutes of placing the detached stem in [2-^{13}C]glycine, and reached a maximum roughly four hours later ($\delta^{13}CO_2$ of roughly 600‰; **Figure 5**). Together with the increase in $^{13}CO_2$ emissions, emissions of [$^{13}C_{1-5}$]isoprene was also stimulated at the expense of [^{12}C]isoprene. After four hours in the [2-^{13}C]glycine solution, relative emissions of [^{12}C]isoprene declined to 42% of total while [$^{13}C_{1-5}$]isoprene increased to values 31, 15, 5, 4, and 3 %, respectively. Thus, a large fraction (51%) of isoprene emissions under [2-^{13}C]glycine contained one to three ^{13}C atoms. This labeling of isoprene was confirmed by GC-MS measurements (data not shown). When the stem was placed back in water, emissions of $^{13}CO_2$ and [$^{13}C_{1-5}$]isoprene quickly decreased to natural abundance levels while [^{12}C]isoprene increased. This result suggests a rapid unlabeling of photorespiratory and isoprene precursor pools, and that [2-^{13}C]glycine delivered to the leaves via the transpiration stream does not accumulate, but is rapidly metabolized.

2.7. Changes in glycine-derived labeling patterns under changing temperature and photorespiratory conditions

Leaf temperature curves with [2-^{13}C]glycine under photorespiratory conditions ($^{12}CO_2$, 50 and 150 ppm) were used to evaluate the temperature dependence of putative photorespiratory carbon incorporation into isoprene and CO_2. Under constant light conditions (1000 µmol m^{-2} s^{-1} PAR), parallel environmental and gas-exchange measurements were made as a function of leaf temperature on single detached shimbillo leaves. Isoprene (PTR-MS) and CO_2 (CRDS) ^{13}C-labeling dynamics were examined. In leaves exposed to photorespiratory conditions (50 ppm $^{12}CO_2$; negative net photosynthesis) and [2-^{13}C]glycine, emissions of labeled $^{13}CO_2$ were observed within minutes of placing the leaf in the solution (**Figure 6a**). $^{13}CO_2$ emissions (0.23-0.26 µmol m^{-2} s^{-1}) remained stable for over ~1 hr while the leaf temperature was maintained at 30 °C and only slightly increased (0.28 µmol m^{-2} s^{-1}) when leaf temperatures were elevated to 35 °C. A decline in $^{13}CO_2$ emissions at higher leaf temperatures was observed (>35 °C); this may be related to increased stomatal resistance and reduced transpiration rates at the higher leaf temperatures (data not shown). This could increase $^{13}CO_2$ photoassimilation rates and reduce [2-^{13}C]glycine uptake rates resulting in decreased $^{13}CO_2$ emissions.

Upon exposure to [2-^{13}C]glycine, the label also rapidly appeared as [$^{13}C_{1-5}$]isoprene within minutes, with [$^{13}C_1$]isoprene and [$^{13}C_2$]isoprene being the dominant species. The labeling pattern of isoprene quickly stabilized with [$^{13}C_{1-3}$]isoprene accounting for 50-55 % of total isoprene emissions and remained stable for over 1 hourr at constant (30 °C) leaf temperature. Although emissions of unlabeled [^{12}C]isoprene were not strongly stimulated by increases in leaf temperature, those of [$^{13}C_{1-3}$]isoprene were. In contrast to $^{13}CO_2$ emissions which declined at the highest leaf temperatures, [$^{13}C_{1-3}$]isoprene continued to increase up to the highest leaf temperature examined (43.0 °C). At 43.0 °C, relative emissions were: [^{12}C]isoprene: 27 %, [$^{13}C_1$]isoprene: 34 %, [$^{13}C_2$]isoprene: 25 %, [$^{13}C_3$]isoprene: 10 %, [$^{13}C_4$]isoprene: 3 %. This contributed to a decrease in [^{12}C]isoprene relative emissions with temperature (27 % at the highest leaf temperature; 43.0 °C). Small emissions of fully ^{13}C-labeled [$^{13}C_5$]isoprene emissions could also be detected up to 32.5 °C leaf temperature (4 %) but returned to background levels at higher leaf temperatures.

The experiment was repeated on leaves under higher, but still photorespiratory, $^{12}CO_2$ concentrations, (150 ppm $^{12}CO_2$). In this case, $^{13}CO_2$ emissions increased with increasing temperature, up to 37.5 °C, where a decline in emissions was observed. Both [^{12}C]isoprene and [$^{13}C_{1-3}$]isoprene increased with increasing temperature throughout the experiment; no decrease was observed (**Figure 6b**). Relative increases in [$^{13}C_{1-3}$]isoprene were greater than increases in [^{12}C]isoprene, resulting in an overall decrease in the relative emissions of [^{12}C]isoprene with temperature to a minimum of 43 % of total emissions at 37.5 °C. At high leaf temperatures, up to 51% of total isoprene emissions had at least one ^{13}C ([$^{13}C_1$]isoprene: 31 %, [$^{13}C_2$]isoprene: 15 %, [$^{13}C_3$]isoprene: 5 %).

3. Discussion

3.1 Coupling of GC-MS, PTR-MS, and CRDS instruments to a leaf photosynthesis system

To finely delineate the contribution of different carbon sources to isoprene under different environmental conditions, we developed a novel analytical approach. The approach is based on the coupling of PTR-MS, thermal desorption GC-MS, and CRDS instruments to a Li-Cor leaf photosynthesis system. Label was provided through $^{12}CO_2$ or $^{13}CO_2$ fumigation, or through transpiration stream feeding with a [2-^{13}C]glycine solution. This system enabled us to observe real-time dynamics of [^{12}C]isoprene and [$^{13}C_{1-5}$]isoprene leaf emissions during light and temperature curves (PTR-MS) while performing ^{13}C-labeling analysis of isoprene fragment and parent ions C_2, C_4, and C_5 (GC-MS). The coupling of both GC-MS and PTR-MS allows us to overcome the limitations of the individual MS systems. PTR-MS only measures signals at a given mass to charge ratio at unit mass resolution, leaving the results with significant uncertainties around the identity of the responsible compound(s). PTR-MS produces real-time emission

data, but cannot discriminate between other compounds with the same nominal molecular mass (e.g. isoprene and furan), or determine the difference between a parent ion or an interfering fragment ion from another compound (e.g. isoprene or a fragment of a C_5 green leaf volatile) (Fall et al., 2001). High light and temperature stresses are known to promote emission of a number of other volatile compounds (Holopainen and Gershenzon, 2010), and these compounds could substantially interfere with the PTR-MS signals attributed to isoprene. As the GC-MS provides chromatographic separation of isoprene from other compounds before mass analysis, this data provides an accurate assessment of isoprene carbon sources as a function of light and temperature that can directly be compared with the PTR-MS data. Moreover, because common commercial infrared gas analyzers have very low and unquantified sensitivity to $^{13}CO_2$, the coupling of the CLDS laser to the photosynthesis system enabled us to measure $^{13}CO_2$ concentrations during isoprene labeling studies and $^{13}CO_2$ photorespiratory emission rates during [2-^{13}]glycine branch and leaf feeding experiments.

3.2 Relative contributions of different carbon sources do not change as a function of light intensity

Following the initiation of $^{13}CO_2$ labeling during light and temperature curves, mango leaves continued to release [^{12}C]isoprene for 20-30 min before the [^{13}C] label began to appear in [$^{13}C_{1-5}$]isoprene (**Figures 1b,c** and **2b,c**). This release may reflect the time required for the fixed [^{13}C] to move through metabolism and appear in isoprene, replacing [^{12}C] in the system. Leaf DMAPP and/or MEP pathway intermediate pools may be relatively high in mango leaves under our experimental conditions. Using $^{13}CO_2$ labeling, we found that relative emissions of [$^{13}C_5$]isoprene (% of total) determined by PTR-MS, isoprene $^{13}C/^{12}C$ isotope ratios (R_2, R_4, and R_5) determined by GC-MS for C_2, C_4, and C_5 ions, and net photosynthesis rates shared the same optimum in response to leaf temperature, and were tightly coupled across all light and temperature conditions studied. Thus, conditions that maximize net photosynthesis rates also maximize the relative emission rates of [$^{13}C_5$]isoprene (% of total). While [$^{13}C_5$]isoprene showed a strong light stimulation in mango leaves, [^{12}C]isoprene emissions remained low and were not stimulated by increases in light (**Figure 1,** supplementary **Figure S1**). Thus, the increased isoprene emission observed under increasing irradiation (PAR > 500 µmol m^{-2} s^{-1}) is due entirely to synthesis from recently-fixed carbon.

3.3 Above the optimum for net photosynthesis, the relative contribution of alternate carbon sources increases

Similarly to the situation under increasing illumination in mango leaves, as temperatures increase to the optimum temperature for net photosynthesis, the increase in net photosynthesis rate is driven by increases in the gross photosynthesis rate, and increases in [$^{13}C_5$]isoprene emissions also occur without significant stimulation in [^{12}C]isoprene emissions (**Figures 2, 3**). However, at leaf temperatures above the optimum

for net photosynthesis, the proportion of carbon derived from alternate carbon sources increased to support high isoprene production rates (**Figures 2, 3**); this is consistent with previous findings in poplar, a temperate tree species (Funk et al., 2004). Consequently, although absolute and relative emissions of [$^{13}C_5$]isoprene were coupled across light curves (**Figure 1,** supplementary **Figure S1**), they became decoupled at high leaf temperatures (**Figures 2** and **3**): absolute emissions of [$^{13}C_5$]isoprene peaked at higher leaf temperatures than the optimum for relative [$^{13}C_5$]isoprene emissions. We observed a similar response in a second tropical species, shimbillo, under similar conditions (**Figure 4b**), suggesting that the response is typical among isoprene-emitting species.

3.4 A rapid mechanism for balancing availability of carbon for isoprene production under sharp temperature changes

In addition to an overall increase in alternate carbon sources at increased leaf temperatures, a striking short-term compensatory response was observed during sharp temperature ramps in mango at temperatures above the optimum for photosynthesis (**Figure 2b,c**). In these instances, sharp decreases in [$^{13}C_5$]isoprene were mirrored by sharp increases in all partially labeled isoprene species. The increase for each species was proportionate to the relative contribution of each species to total isoprene emission. This response was also observed in shimbillo leaves under similar conditions (**Figure 4b**), although it was not quite as pronounced as the mango response. These data suggest that when photosynthesis is unable to provide sufficient substrate to maintain isoprene production during temperature shifts, a rapid mechanism exists to compensate *via* carbon from alternative sources.

Isoprene synthase (IspS) is responsible for conversion of DMAPP to isoprene (Silver and Fall, 1991). While DMAPP is found both in the cytosol (from MVA pathway flux) and the chloroplast (from MEP pathway flux), IspS is localized in the chloroplast (Wildermuth and Fall, 1996; Schnitzler et al., 2005; Vickers et al., 2010), so can only use DMAPP from the chloroplastic pool. Leaf isoprene emission is directly correlated with extractible enzyme activity (Monson et al., 1992) as well as with the amount of IspS in the leaf (Vickers et al., 2010), and IspS levels do not change rapidly in response to changing environmental conditions (Vickers et al., 2011), suggesting that the enzyme itself is not under direct regulation and isoprene production is largely driven by the availability of DMAPP in the chloroplast. Under the assumption that isotopic discrimination by IspS is trivial, we can presume that the decrease in the amount of labeled isoprene observed during temperature ramps is a result of a transient decrease in photosynthetically-supplied label, and consequently a decrease in photosynthesis-derived MEP pathway flux. The speed of the compensatory response observed in **Figure 2** (essentially instantaneous) suggests that an alternative (unlabeled) carbon source is immediately available to the isoprene synthase (IspS)

enzyme. This alternative source of carbon may derive from rapid import of glycolysis and/or MVA intermediates (pyruvate/PEP and IPP/DMAPP) from the cytosol and/or from chloroplastic production of unlabeled MEP pathway precursors (pyruvate and G3P). Unlabeled chloroplastic MEP pathway precursors may be generated during photorespiration, starch degradation, and the reassimilation of respiratory and photorespiratory CO_2.

Although it is demonstrated that cross-talk exists between the MVA and MEP pathways (Laule et al., 2003), the degree and direction of cross-talk is highly variable between species/tissues/developmental stages etc. Complex and poorly understood regulatory mechanisms exist in plants to ensure that sufficient isoprenoid precursors are available for synthesis of isoprenoid compounds (Rodríguez-Concepción, 2006). It has been shown that prenyl phosphates can be transported across the chloroplast membrane (Flügge and Gao, 2005a) and, while it is generally thought that cross-talk at the prenyl phosphate level occurs at only low levels under normal circumstances, it is clear that exchange of prenyl phosphates between compartments occurs at relatively high levels in a variety of circumstances, in particular, where production of high levels of specific isoprenoids is required (Rodríguez-Concepción, 2006). However, the rate of cross-talk has not been accurately quantified.

3.5 Investigating photorespiration as a source of alternate carbon for isoprene production

Both recently assimilated and "alternate" carbon sources are known to contribute to isoprene production in plants, and the relative contribution of different carbon sources changes under changes in environmental conditions - in particular, drought, salt and heat stress (Loreto and Delfine, 2000; Funk et al., 2004; Brilli et al., 2007), and changes in CO_2/O_2 ratios (Jones and Rasmussen, 1975; Karl et al., 2002b; Trowbridge et al., 2012). These former stresses can increase stomatal resistance resulting in reduced CO_2/O_2 ratios, decreasing rates of net photosynthesis while increasing photorespiratory rates (Wingler et al., 1999; Hoshida et al., 2000). These patterns may be reflected in changes in relative contributions of photosynthetic and alternate carbon sources for isoprene when the flux of immediately-fixed carbon is limited (sometimes severely). However, alternate carbon sources for isoprene are relatively poorly defined and little is known about how they vary during changes in light and temperature, the environmental variables known to have the largest effect on isoprene emissions.

One potential source for the unlabeled isoprene carbon is photorespiration. High temperatures and low CO_2 concentrations are well known to stimulate photorespiration at the expense of photosynthesis, resulting in a decline of net photosynthesis rates (Bauwe et al., 2010; Hagemann et al., 2013). Under increased temperature, the enzyme Ribulose-1,5-bisphosphate carboxylase/oxygenase (RuBisCO) is less

able to discriminate between CO_2 and O_2; moreover, the solubility of CO_2 is also reduced, thereby resulting in an increase in the relative concentration of O_2, to CO_2. Consequently, photorespiration increases at increasing temperatures. This makes photorespiration an interesting potential source of alternate carbon under the experimental conditions used here.

It was proposed 40 years ago that photorespiration could serve as an important alternate carbon source for isoprene (Jones and Rasmussen, 1975). In this research study, strong radioactivity was observed in isoprene from leaf slices incubated with [2-^{14}C]glycine, a photorespiratory intermediate (**Figure 7**). The authors noted striking parallels between known controls over isoprene emissions and photorespiration rates, including a stimulation of both processes by temperature and low CO_2 concentrations, and suppression by high CO_2 concentrations. Prior to the current study, evidence that photorespiratory intermediates could contribute to isoprenoid production in chloroplasts had already been published (Shah and Rogers, 1969). This study demonstrated the appearance of radioactive label in MEP pathway products (including β-carotene during exposure of excised shoots to [2-^{14}C]glyoxylate and [U-^{14}C]serine, both photorespiratory intermediates). However, subsequent studies suggested that there was no close relationship between isoprene emissions and photorespiration (Monson and Fall, 1989; Hewitt et al., 1990; Karl et al., 2002b). Most of these studies used reduced oxygen mixing ratios to inhibit photorespiratory rates; however, this may also interfere with mitochondrial respiration and stimulate fermentation and the accumulation of pyruvate - a substrate for isoprene production (Kimmerer and Macdonald, 1987; Vartapetian and Jackson, 1997; Vartapetian et al., 1997). Thus, low oxygen mixing ratios may stimulate isoprene production through an increased import of pyruvate into chloroplast (Jardine et al., 2010).

Assuming absolute [$^{13}C_5$]isoprene emission reflects gross photosynthesis rates while relative emissions reflect net photosynthesis rates, the observed uncoupling of isoprene emission from net photosynthesis is likely influenced by the high temperature and/or low CO_2/O_2 stimulation of respiratory (Loreto et al., 2004) and photorespiratory (Jones and Rasmussen, 1975) CO_2 production. While well-known to reduce net photosynthesis rates, these processes may potentially act as alternate carbon sources for isoprene. During $^{13}CO_2$ labeling, emissions of [^{12}C]isoprene and partially labeled [$^{13}C_{1\text{-}4}$]isoprene, representing alternate carbon sources, increased with leaf temperature. For example, at leaf temperatures of 45 °C, up to 80% of isoprene was emitted as [^{12}C]isoprene and [$^{13}C_{1\text{-}4}$]isoprene compared with up to 41% at the optimal temperature for net photosynthesis (**Figure 3c**). These observations are consistent with previous studies demonstrating increases in alternate carbon contributions for isoprene under conditions known to limit net photosynthesis, including low CO_2 concentrations and drought (Affek and Yakir, 2003; Funk et

al., 2004; Trowbridge et al., 2012). In addition to conditions that limit net photosynthesis, those that enhance the rates of alternate carbon sources (e.g. low CO_2 and high temperature stimulation of photorespiration) may also be important contributors to reduced ^{13}C-labeling of isoprene under $^{13}CO_2$.

We decided to examine photorespiration as a potential carbon source more closely using shimbillo, a species more amenable to transpiration stream feeding. We first repeated the thermal stress experiments under a range of $^{13}CO_2$ concentrations (**Figure 4**). Under photorespiratory conditions (150 ppm $^{13}CO_2$), a reduction in the leaf temperature where emissions of [$^{13}C_5$]isoprene were replaced by partially labeled and unlabeled isoprene was observed (27.5 °C under 150 ppm $^{13}CO_2$ versus 30 °C under 300 ppm $^{13}CO_2$). In contrast, under photosynthetic conditions (800 ppm $^{13}CO_2$), a dramatic increase in the leaf temperature where [$^{13}C_5$]isoprene emissions transitioned to unlabeled or partially labeled isoprene emissions was observed (42.0 °C).

Although photorespiratory intermediates can be labeled during photosynthesis under $^{13}CO_2$, mass spectrometry studies attempting to partition photosynthesis and photorespiration have shown that it is incomplete, likely due to metabolic connections of photorespiratory intermediates with other pathways (Haupt-Herting et al., 2001). Thus under $^{13}CO_2$, if photorespiratory carbon sources begin to dominate photosynthetic carbon sources for Calvin cycle intermediates, then reduced ^{13}C-labeling of isoprene would be expected.

3.6 [2-^{13}C]glycine labeling studies support photorespiration as an alternative carbon source for isoprene

Upon feeding of shimbillo with [2-^{13}C]glycine, we observed a rapid incorporation of label into isoprene and CO_2 (**Figures** 5 and **6**). The results of the shimbillo leaf temperature curves under [2-^{13}C]glycine labeling provide new evidence that both direct (substrate) and indirect (CO_2 re-assimilation) photorespiratory carbon processes contribute to isoprene biosynthesis. During photorespiration, the C_1 of glycine is decarboxylated while the C_2 is used to methylate a second glycine to form serine via a $^{13}CH_2$-tetrahydrofolate intermediate. Thus, the rapid emission of $^{13}CO_2$ and isoprene with multiple ^{13}C atoms (1-5) demonstrates that the supplied [2-^{13}C]glycine can undergo several photorespiratory cycles. For example, [2,3^{13}C]serine could form when the supplied [2-^{13}C]glycine is methylated by $^{13}CH_2$-tetrahydrofolate generated from another [2-^{13}C]glycine. The release of photorespiratory $^{13}CO_2$ emissions would require the formation of glycine with a ^{13}C atom in the first carbon position ([1-^{13}C]glycine) which could occur through the entry of photorespiratory intermediates into the Calvin cycle (e.g. glycerate-3-phosphate, GA3P) followed by the exit of the glycine precursor glycolate into photorespiration. Thus,

emissions of $^{13}CO_2$ from shimbillo leaves under [2-^{13}C]glycine provides evidence of rapid integration of photorespiratory and Calvin cycle intermediates. The output of GA3P from the Calvin cycle with 1-3 ^{13}C atoms could then explain the ^{13}C-labeling patterns observed in isoprene emissions. However, as $^{13}CO_2$ emissions were also observed, re-assimilation of photorespiratory carbon could also be an important source of ^{13}C in isoprene. When ^{13}C emissions in $^{13}CO_2$ was quantitatively compared with ^{13}C emissions in [$^{13}C_{1\text{-}5}$]isoprene under [2-^{13}C]glycine leaf feeding during high leaf temperatures, 10-50 % of ^{13}C emitted as $^{13}CO_2$ was emitted as [$^{13}C_{1\text{-}5}$]isoprene. Interpretation of these results however is complicated by the reduced transpiration rates and stomatal conductance at high leaf temperatures leading to a decreased uptake rate of the [2-^{13}C]glycine solutions and potentially increased reassimilation of $^{13}CO_2$. Nonetheless, our observations present new evidence that the photorespiratory C_2 cycle and the photosynthetic C_3 Calvin cycle are intimately connected to the MEP pathway for alternate and photosynthetic carbon sources for isoprenoid biosynthesis (**Figure 7**).

4. Conclusions

In this study, we show for the first time real-time responses of photosynthetic and alternate carbon sources for isoprene synthesis under variations in light and temperature. We also show that one possible alternate carbon source for isoprene precursors is photorespiration which is known to become active at the expense of photosynthesis under high temperatures and contribute to the decline in net photosynthesis. While previous research on the effects of CO_2 concentrations on isoprene carbon sources have focused on its potential effects on carbohydrate metabolism (Trowbridge et al., 2012), our results provide new data supporting its role in influencing photorespiratory carbon sources for isoprene. These data support the original suggestion of Jones and Rasmussen (1975), and stand in contrast to studies in the interim that have suggested photorespiration does not provide an alternate carbon source for isoprene.

The processes described here could help maintain the carbon flux through the MEP pathway under high temperature conditions. This may help maintain the biosynthesis of isoprene (and possibly other isoprenoids including photosynthetic pigments) under stress conditions that reduce photosynthesis rates while increasing photorespiratory rates. Given that the highest isoprene emission rates occur under these conditions, the investment of alternate carbon sources into isoprene biosynthesis is considerable, but may be important for helping to protect the photosynthetic machinery from oxidative damage and the activation of stress-related signaling processes (Vickers et al., 2009a; Karl et al., 2010; Loreto and Schnitzler, 2010; Jardine et al., 2013; Vickers et al., 2014). By including the representation of photosynthetic and photorespiratory carbon sources of isoprene at high temperatures in mechanistic Earth System Models (ESMs), this study could aid in improving the links between terrestrial carbon metabolism, isoprene emissions, and atmospheric chemistry and improve estimates of the terrestrial carbon budget.

5. Materials and Methods

5.1 Isoprene emissions and net photosynthesis

At the Lawrence Berkeley National Laboratory (LBNL) in Berkeley, California, three growth chambers (E36HO, Percival Scientific, USA) were used to acclimatize 9 dwarf mango (*Mangifera indica;* Linneaus cultivar: Nam Doc Mai, Top Tropicals, USA) plants for four weeks prior to experimentation. This tropical species was selected because of its high reported emissions of isoprene (Jardine et al., 2012a; Jardine et al., 2013) and the relative ease of obtaining potted plants from a commercial supplier. The plants were maintained under photosynthetically active radiation (PAR) flux density of 300-1500 μmol m^{-2} s^{-1}

(depending on leaf height) with a light period of 7:00 to 17:59, light/dark air temperatures of 30/28 °C and ambient CO_2 concentrations of 400 ppm. The plants were grown in 7.6 L plastic pots (8.5″ diameter) plastic pots filled with peat moss soil and watered weekly. Light and temperature curves were carried out on intact individual leaves under $^{12}CO_2$ and $^{13}CO_2$ as described in section 5.2 below.

Net photosynthesis and isoprene emission rates were quantified from mango leaves using a commercial leaf photosynthesis system (LI-6400XT, LI-COR Inc., USA) interfaced with a high sensitivity quadrupole proton transfer reaction mass spectrometer (PTR-MS, Ionicon Analytik, Austria) and a gas chromatograph-mass spectrometer (GC-MS, 5975C series, Agilent Technologies, USA). Gas samples were collected on thermal desorption tubes (TD) and injected into the GC-MS for analysis using an automated TD system (TD100, Markes International, UK) as described in section 5.4 below. All tubing and fittings employed downstream of the leaf chamber were constructed with PFA Teflon (Cole Parmer, USA) to prevent isoprene adsorption. Ultrahigh purity hydrocarbon free air from a zero air generator (737, Pure Air Generator, AADCO Instruments, USA) was humidified with a glass bubbler filled with distilled water and directed to the LI6400XT gas inlet via an overblown tee. At all times, the flow rate of air into the leaf chamber was maintained at 537 ml/min, the internal fan was set to the maximum speed, and the CO_2 concentration entering the chamber was maintained at 400 ppm. Using a four-way junction fitting, air exiting the leaf chamber was delivered to the PTR-MS (40 ml/min) and the TD tube (100 ml/min when collecting) with the remainder of the flow diverted to the vent/match valve within the LI6400XT. The excess flow entering the vent/match valve was maintained to at least 200 ml/min by loosely tightening the chamber onto the leaf using the tightening nut.

One leaf from each of 4 mango plants was used to evaluate the response of net photosynthesis and isoprene emissions to changes in PAR and leaf temperature; each curve was generated by averaging the results from the 4 leaves. Each day of the study for either a PAR or leaf temperature response curve, one leaf near the top of one of the plants was placed in the enclosure and either leaf temperature or PAR was independently varied while the other variable was held constant. To prevent artificial disturbance to the plants, during gas exchange measurements the LI6400XT leaf cuvette was placed inside the growth chamber with the plants. Before and after each PAR and leaf temperature curve, background measurements were collected with an empty leaf cuvette. During these background measurements, two TD tube samples were collected with PAR/leaf temperature conditions identical to the first and last values, respectively in the series. Before and after the introduction of the leaf into the cuvette, continuous isoprene emission rates were acquired using PTR-MS.

For light response curves, measurements were made under constant leaf temperature (30 °C) at PAR flux of 0, 25, 50, 75, 100, 250, 500, 1000, 1500, and 2000 µmol m^{-2} s^{-1}. For leaf temperature response curves, measurements were made under constant irradiance (1000 µmol m^{-2} s^{-1}) at 25, 27.5, 30, 32.5, 35, 37.5, 40, and 42 °C. In some cases, higher leaf temperatures up to 44-45 °C could also be reached. Control experiments were also conducted (2 leaves randomly selected from one plant) with the same temperature levels but in the dark (0 µmol m^{-2} s^{-1}) to evaluate the potential for isoprene emissions in the absence of light at elevated temperatures. Following the establishment of a new PAR or leaf temperature level, a delay of 5 minutes was used prior to data logging to allow the trace gas fluxes to stabilize. After the delay, the reference and sample infrared gas analyzers were matched, leaf environmental and physiological variables were logged, and isoprene emissions were collected on a TD tube (10 minutes collections for temperature curves and 5 minute collections for PAR curves).

5.2 $^{13}CO_2$ labeling in mango

During ^{13}C-labelling of isoprene emissions from mango leaves, a cylinder with 99% $^{13}CO_2$ (Cambridge Scientific, USA) was connected to the LI-6400XT. In order to maintain a constant ~400 ppm $^{13}CO_2$ in the reference air entering the leaf cuvette, the CO_2 concentration in the reference chamber was set to 100 ppm. The difference between $^{13}CO_2$ concentration as measured by LI-6400XT and the CO_2 concentration setpoint is due to the reduced sensitivity of the LI-6400XT detector to $^{13}CO_2$ relative to $^{12}CO_2$ (roughly 25 %). While this configuration allowed for ^{13}C-labeling of isoprene, an accurate measurement of net photosynthesis could not be obtained, due to the reduced sensitivity for $^{13}CO_2$. Therefore, we compared ^{13}C-labeling patterns of isoprene as a function of PAR and leaf temperature with isoprene emissions and net photosynthesis under $^{12}CO_2$. PAR and leaf temperature curves under $^{13}CO_2$ were conducted using the method described above for $^{12}CO_2$ and a total of 4 PAR and 4 leaf temperature curves were carried out (4 different leaves on one plant).

5.3 Photorespiratory carbon sources analysis of isoprene using $^{13}CO_2$ and [2-^{13}C]glycine labeling

To evaluate the potential for photorespiratory carbon sources for isoprene, five naturally occurring 5-10 m tall *Inga edulis* (shimbillo) trees growing near the laboratory at the National Institute for Amazon Research (INPA) in Manaus, Brazil were used. This species was selected because detached shimbillo leaves maintained high transpiration rates, and therefore uptake of the [2-^{13}C]glycine solutions, for at least 12 hours following leaf detachment from the tree. In contrast, mango leaves showed greatly reduced transpiration rates within 1.0 hour following leaf detachment from the tree. Temperature curves (25.0, 27.5, 30.0, 32.5, 35.0, 37.5, 40.0, 42.5 °C) were carried out under three different $^{13}CO_2$ concentrations (150, 300, 800 ppm) on attached fully expanded shimbillo leaves (3 leaves at each $^{13}CO_2$ concentration). For [2-^{13}C]glycine labeling experiments, the stem of detached shimbillo branchlets (2.7-3.2 gdw) were

placed in the [2-^{13}C]glycine solution and the leaves were sealed in a 4.0 L Teflon branch enclosure under constant light (300-500 µmol m^{-2} s^{-1} PAR) and air temperature conditions (28-30 °C) and with 2.0 L min^{-1} of hydrocarbon free air flowing through. Isoprene and CO_2 labeling analysis were performed using PTR-MS, GC-MS, and a cavity ringdown spectrometer for isotopic CO_2 (CRDS model G2201-I, Picarro Inc.). Three replicate branchlet labeling experiments were performed on successive days. In addition, temperature curves (30.0, 32.5, 35.0, 37.5, 40.0, 42.5 °C) were carried out on three detached shimbillo leaves fed with 10 mM [2-^{13}C]glycine via the transpiration stream. Detached leaves were placed in tap water before being recut, transported to the laboratory, and placed in the [2-^{13}C]glycine solution. The upper portion of the leaf was then immediately placed in the LI-6400XT leaf chamber at 1000 µmol m^{-2} s^{-1} PAR and with 537 ml/min humidified air flowing through. Two leaves were measured under 50 ppm $^{12}CO_2$ and two leaves were measured under 150 ppm $^{12}CO_2$ entering the leaf chamber. In addition to leaf physiological variables (e.g. net photosynthesis, transpiration, etc.) measured by the LI-6400XT, [^{12}C]isoprene and [$^{13}C_{1-5}$]isoprene emissions were measured using PTR-MS in parallel with $^{13}CO_2$ emissions using CRDS.

5.4 Thermal desorption gas chromatography-mass spectrometry (GC-MS)

Isoprene in leaf enclosure air samples were collected by drawing 100 sccm of enclosure air through a TD tube for 5 or 10 minutes (0.5 and 1.0 L, respectively) by connecting a mass flow controller and a pump downstream of the tube. TD tubes were purchased commercially, filled with Tenax TA, Carbograph 1TD, and Carboxen 1003 adsorbents (Markes International, UK). The TD tube samples were analyzed for isoprene with a TD-100 thermal desorption system (Markes International, UK) interfaced to a gas chromatograph/electron impact mass spectrometer with a triple-axis detector (5975C series, Agilent Technologies, USA). After loading a tube in the TD-100 thermal desorption system, the collected samples were dried by purging for 4 minutes with 50 sccm of ultra-high purity helium (all flow vented out of the split vent) before being transferred (290 ^{o}C for 5 min with 50 sccm of helium) to the TD-100 cold trap (air toxics) held at 0 ^{o}C. During GC injection, the trap was heated to 290°C for 3 min while back-flushing with carrier gas at a flow of 6.0 sccm. Simultaneously, 4.0 sccm of this flow was directed to the split and 2.0 sccm was directed to the column (Agilent DB624 60 m x 0.32 mm x 1.8 µm). The oven temperature was programmed with an initial hold of 3 min at 40 °C followed by an increase to 88 °C at 6 °C min^{-1} followed by a hold at 230 °C for 10 min. The mass spectrometer was configured for trace analysis with a 15 times detector gain factor and operated in scan mode (m/z 35-150). Identification of isoprene from TD tube samples was confirmed by comparison of mass spectra with the U.S. National Institute of Standards and Technology (NIST) mass spectral library and by comparison of mass spectra and retention time with an authentic liquid standard (10 µg/ml in methanol, Restek, USA). The GC-MS was calibrated to isoprene by injecting 0.0, 0.5, 1.0, and 2.0 µl of the liquid standard onto separate TD tubes with 100 ml min^{-1} of

ultrahigh purity nitrogen flowing through for 15 min (calibration solution loading rig, Markes International, UK).

The thermal desorption GC-MS analysis method for ^{13}C-labeled isoprene emissions from mango leaves exposed to $^{13}CO_2$ was identical to those under $^{12}CO_2$ except for the parameters of the mass spectrometer. For $^{13}CO_2$ experiments, the mass spectrometer was also configured for trace analysis with a 15 times detector gain factor but operated in selected ion monitoring mode with 18 different m/z values measured sequentially with a 20 ms dwell time each. These include m/z 27-29 (C_2 isoprene fragment, 0-2 ^{13}C atoms respectively), m/z 53-57 (C_4 isoprene fragment, 0-4 ^{13}C atoms respectively), and m/z 68-73 (C_5 isoprene parent ion, 0-5 ^{13}C atoms respectively). $^{13}C/^{12}C$ isotope ratios (R) for each sample were calculated for C_2 ($^{13}C_2H_3/^{12}C_2H_3$, R_2 = m/z 29/27) and C_4 ($^{13}C_4H_5/^{12}C_4H_5$, R_4 = m/z 57/53) fragment ions as well as C_5 ($^{13}C_5H_8/^{12}C_5H_8$, R_5 = m/z 73/68) parent ions. It is important to note that R_2, R_4, and R_5 can currently only be considered qualitative indicators of isoprene ^{13}C-labeling intensity. This is because just downstream of each GC-MS ^{12}C-fragment and parent ion (m/z 27, 53, 68), additional fragments exist, produced for example, by hydrogen abstractions. ^{13}C-labeling of these downstream fragments may increase the signals assumed to be only due to ^{12}C-ions (m/z 27, 53, 68). This may result in an under-prediction of R_2, R_4, and R_5 which was not accounted for.

5.5 Proton Transfer Reaction Mass Spectrometry (PTR-MS)

Isoprene emissions were analyzed from the LI6400XT leaf cuvette in real-time using a PTR-MS operated with a drift tube voltage of 600 V, temperature of 40 °C, and pressure of 200 Pa. The following mass to charge ratios (m/z) were monitored during each PTR-MS measurement cycle: 21 ($H_3{}^{18}O^+$), 32 ($O_2{}^+$) with a dwell time of 20 ms each, and 37 (H_2O-H_3O^+) with a dwell time of 2 ms. Routine maintenance prior to the measurement campaign in California, USA and Manaus, Brazil (ion source cleaning and detector replacement) enabled the system to generate H_3O^+ at high intensity (1.5-2.5 10^7 cps H_3O^+) and purity ($O_2{}^+$ and H_2O-H_3O^+ < 5% of H_3O^+). During each measurement cycle, the protonated parent ion of [^{12}C]isoprene was measured at m/z 69 with a 2 s dwell time. During ^{13}C-labeling studies, ^{13}C-labeled parent ions of isoprene were also measured with a 2 s dwell time and include m/z 70 [$^{13}C_1$]isoprene, m/z 71 [$^{13}C_2$]isoprene, m/z 72 [$^{13}C_3$]-isoprene, m/z 73 [$^{13}C_4$]-isoprene, and m/z 74 [$^{13}C_5$]isoprene. The PTR-MS was calibrated using 1.0 ppm of isoprene gas standard (ozone precursors, Restek Corp, USA) diluted in humidified zero air to six concentrations between 0 and 10.5 ppb. The PTR-MS sensitivity to [$^{13}C_{1-5}$]isoprene (m/z 70-74) was assumed to be identical to that measured for [^{12}C]isoprene (m/z 69, 74 cps/ppb).

6. Supplementary Information

An additional figure can be found in the supporting information; **Figure S1**: GC-MS ^{13}C-labeling analysis of isoprene emissions from 4 mango leaves during photosynthesis under $^{13}CO_2$ as a function of PAR.

7. Acknowledgements

This research was supported by the Office of Biological and Environmental Research of the U.S. Department of Energy under Contract No. DE-AC02-05CH11231 as part of their Terrestrial Ecosystem Science Program and the National Science Foundation CHE0216226. The authors would like to kindly acknowledge the advice and support of Sebastien Biraud, Sara Hefty, Ron Woods, and Rosie Davis at Lawrence Berkeley National Laboratory in this project. Logistical support from the Large Biosphere-Atmosphere (LBA) and Green Ocean Amazon (GoAmazon) project in Manaus, Brazil is also acknowledged.

8. Figure Legends

Figure 1: Dependencies of net photosynthesis (Pn) and isoprene emission rates from mango leaves on PAR intensities at a constant leaf temperature (30 °C). **a**) Average of leaf isoprene emissions (GC-MS; blue) and net photosynthesis rates (green) as a function of PAR from four mango leaves. Shaded areas represent +/- one standard deviation. Also shown are representative PTR-MS time series plots showing the influence of increasing PAR intensity on the dynamics of **b**) absolute emissions and **c**) relative emissions (% of total) of [^{12}C]isoprene and [$^{13}C_{1\text{-}5}$]isoprene from a single mango leaf during photosynthesis under $^{13}CO_2$. Vertical dashed lines represent optimum temperatures for net photosynthesis (Pn_{max}) and isoprene emissions (I_{max}).

Figure 2: Dependencies of net photosynthesis (Pn) and isoprene emission rates from mango leaves on leaf temperature under constant illumination (PAR of 1000 µmol m^{-2} s^{-1}). **a**) Average leaf isoprene emissions (GC-MS) and net photosynthesis rates as a function of leaf temperature from 4 mango leaves. Shaded areas represent +/- one standard deviation. Also shown are representative PTR-MS time series plots showing the influence of increasing leaf temperature on the dynamics of **b**) absolute emissions of [^{12}C]isoprene and [$^{13}C_{1\text{-}5}$]isoprene and **c**) relative isoprene isotopologue emissions rates (% of total) from a single mango leaf during photosynthesis under $^{13}CO_2$. Arrows indicate periods of rapid of ^{13}C-depletion of isoprenoid intermediates followed by re-enrichment. Vertical dashed lines represent optimum temperature ranges for net photosynthesis (Pn_{max}) and isoprene emissions (I_{max}).

Figure 3: GC-MS ^{13}C-labeling analysis of isoprene emissions from 4 mango leaves during photosynthesis under $^{13}CO_2$ as a function of leaf temperature. **a**) Structure of isoprene GC-MS fragment ions with two carbon atoms (C_2, red) and four carbon atoms (C_4, blue) together with the isoprene parent ion with five carbon atoms (C_5, green). Carbon atoms derived from glyceraldehyde-3-phosphate (GA3P) and pyruvate are shown as *C and C respectively. **b**) Average $^{13}C/^{12}C$ isoprene emission ratios (R) of C_2 ($^{13}C_2/^{12}C_2$, R_2 = m/z 29/27) and C_4 ($^{13}C_4/^{12}C_4$, R_4 = m/z 57/53) fragment ions and C_5 ($^{13}C_5/^{12}C_5$, R_5 = m/z 73/68) parent ions. **c**) Average emission rates for [^{12}C]isoprene (m/z 68) and [$^{13}C_5$]isoprene (m/z 73) normalized to the

maximum emissions of [$^{13}C_5$]isoprene. Vertical dashed lines represent optimum temperature ranges for net photosynthesis (Pn_{max}) and isoprene emissions (I_{max}).

Figure 4: Representative PTR-MS time series plots showing absolute and relative emissions (% of total) of [^{12}C]isoprene and [$^{13}C_{1-5}$]isoprene as a function leaf temperature from three separate shimbillo leaves exposed to (**a**) 150, (**b**) 300, and (**c**) 800 ppm $^{13}CO_2$. Note that increased $^{13}CO_2$ concentrations strongly enhance the temperature corresponding to the maximum relative emissions of [$^{13}C_5$]isoprene (150 ppm: 27.5 °C, 300 ppm: 30.0 °C, 800 ppm: 42.0 °C).

Figure 5: Representative CRDS and PTR-MS time series plot showing ^{13}C-labeling of photorespiratory CO_2 and isoprene during 10 mM [2-^{13}C]glycine feeding of a detached shimbillo branch through the transpiration stream under constant light (300-500 µmol m^{-2} s^{-1} PAR) and air temperature (28-30 °C). The detached branch was first placed in water, then transfered to the [2-^{13}C]glycine solution for four hours, before being replaced in water.

Figure 6: Representative CRDS and PTR-MS time series plots showing the influence of increasing leaf temperature on absolute emissions of photorespiratory $^{13}CO_2$, [^{12}C]isoprene and [$^{13}C_{1-5}$]isoprene from detached shimbillo leaves in a 10 mM [2-^{13}C]glycine solution under (a) 50 ppm $^{12}CO_2$ and (b) 150 ppm $^{12}CO_2$. Also shown are the relative emissions (% of total) of [^{12}C]isoprene and [$^{13}C_{1-5}$]isoprene. Note the general pattern of increasing relative emissions of [$^{13}C_{1-4}$]isoprene and a decrease in [^{12}C]isoprene with temperature.

Figure 7: Simplified schematic of isoprenoid metabolism in photosynthetic plant cells and its relationship to photosynthesis, glycolysis, respiration, and photorespiration. Although the mevalonate (MVA) pathway is found in the cytosol and the methylerythritol phosphate (MEP) pathway is found in the chloroplast, some cross-talk occurs between the pathways through the exchange of intermediates (dashed arrows). CO_2 assimilated by the Calvin Cycle, entering the MEP pathway as GA3P, and ending up as carbon atoms 1-3 of isoprene are shown in green. Metabolite abbreviations include: Acetyl-CoA: acetyl-coenzyme A, AA-CoA: acetoacetyl-coenzyme A, CTP: cytidine 5' triphosphate, CDMEP: 4-(cytidine 5'-diphospho)-2-C-methyl-D-erythritol, CMP: cytidine 5'monophosphate, DMAPP: dimethylallyl pyrophosphate, DXP: 1-deoxy-D-xylulose-5-phosphate, FPP: farncyl pyrophosphate, GA3P: D-glyceraldehyde 3-phosphate, GPP: geranyl pyrophosphate, GGPP: geranyl geranyl pyrophosphate, G6P: glucose-6-phosphate, HMBPP: 1-hydroxy-2-methyl-2-(E)-butenyl 4-diphosphate, HMG-CoA: (S)-3-hydroxy-3-methylglutaryl-coenzyme A, IPP: isopentenyl pyrophosphate, MECPP: 2-C-methyl-D-erythritol-2,4-cyclodiphosphate, MEP: 2-C-methyl-D-erythritol-4-phosphate, MVA: (R)-mevalonate, MVAP: mevalonate-5-phosphate, MVADP: mevalonate diphosphate, PEP: phospho*enol*pyruvate, PCPPME: 2-phospho-4-(cytidine 5'-diphospho)-2-C-methyl-D-erythritol, Phytyl-PP: phytyl pyrophosphate. Figure modified from Vickers et al., 2009a and Vickers et al., 2014.

9.0 References

Affek HP, Yakir D (2002) Protection by isoprene against singlet oxygen in leaves. Plant Physiology **129:** 269-277

Affek HP, Yakir D (2003) Natural abundance carbon isotope composition of isoprene reflects incomplete coupling between isoprene synthesis and photosynthetic carbon flow. Plant Physiology **131:** 1727-1736

Atkinson R, Arey J (2003) Gas-phase tropospheric chemistry of biogenic volatile organic compounds: a review. Atmospheric Environment **37:** S197-S219

Bauwe H, Hagemann M, Fernie AR (2010) Photorespiration: players, partners and origin. Trends in Plant Science **15:** 330-336

Brilli F, Barta C, Fortunati A, Lerdau M, Loreto F, Centritto M (2007) Response of isoprene emission and carbon metabolism to drought in white poplar (Populus alba) saplings. New Phytologist **175:** 244-254

Delwiche CF, Sharkey TD (1993) Rapid Appearance of C-13 in Biogenic Isoprene When (Co2)-C-13 Is Fed to Intact Leaves. Plant Cell and Environment **16:** 587-591

Fall R, Karl T, Jordon A, Lindinger W (2001) Biogenic C_5 VOCs: release from leaves after freeze-thaw wounding and occurrence in air at a high mountain observatory. Atmospheric Environment **35:** 3905-3916

Flügge UI, Gao W (2005a) Transport of isoprenoid intermediates across chloroplast envelope membranes. Plant Biology **7:** 91-97

Flügge UI, Gao W (2005b) Transport of isoprenoid intermediates across chloroplast envelope membranes. Plant Biology (Stuttgart, Germany)**:** 91-97

Fortunati A, Barta C, Brilli F, Centritto M, Zimmer I, Schnitzler JP, Loreto F (2008) Isoprene emission is not temperature-dependent during and after severe drought-stress: a physiological and biochemical analysis. The Plant Journal **55:** 687-697

Fuentes J, Wang D, Gu L (1999) Seasonal variations in isoprene emissions from a boreal aspen forest. Journal of Applied Meteorology **38:** 855-869

Funk JL, Mak JE, Lerdau MT (2004) Stress-induced changes in carbon sources for isoprene production in Populus deltoides. Plant Cell and Environment **27:** 747-755

Goldstein AH, Goulden ML, Munger JW, Wofsy SC, Geron CD (1998) Seasonal course of isoprene emissions from a midlatitude deciduous forest. Journal of Geophysical Research: Atmospheres (1984–2012) **103:** 31045-31056

Guenther A, Karl T, Harley P, Wiedinmyer C, Palmer P, Geron C (2006) Estimates of global terrestrial isoprene emissions using MEGAN (Model of Emissions of Gases and Aerosols from Nature). Atmospheric Chemistry & Physics **6**

Hagemann M, Fernie AR, Espie GS, Kern R, Eisenhut M, Reumann S, Bauwe H, Weber APM (2013) Evolution of the biochemistry of the photorespiratory C2 cycle. Plant Biology **15:** 639-647

Harley P, Guenther A, Zimmerman P (1996) Effects of light, temperature and canopy position on net photosynthesis and isoprene emission from sweetgum (Liquidambar styraciflua) leaves. Tree Physiology **16:** 25-32

Harley P, Vasconcellos P, Vierling L, Pinheiro CCD, Greenberg J, Guenther A, Klinger L, De Almeida SS, Neill D, Baker T, Phillips O, Malhi Y (2004) Variation in potential for isoprene emissions among Neotropical forest sites. Global Change Biology **10:** 630-650

Haupt-Herting S, Klug K, Fock HP (2001) A new approach to measure gross CO2 fluxes in leaves. Gross CO2 assimilation, photorespiration, and mitochondrial respiration in the light in tomato under drought stress. Plant Physiology **126:** 388-396

Hewitt CN, Monson RK, Fall R (1990) Isoprene Emissions from the Grass Arundo-Donax L Are Not Linked to Photorespiration. Plant Science **66:** 139-144

Holopainen JK, Gershenzon J (2010) Multiple stress factors and the emission of plant VOCs. Trends in Plant Science **15:** 176-184

Hoshida H, Tanaka Y, Hibino T, Hayashi Y, Tanaka A, Takabe T, Takabe T (2000) Enhanced tolerance to salt stress in transgenic rice that overexpresses chloroplast glutamine synthetase. Plant molecular biology **43:** 103-111

Jardine K, Abrell L, Jardine A, Huxman T, Saleska S, Arneth A, Monson R, Karl T, Fares S, Loreto F, Goldstein A (2012a) Within-plant isoprene oxidation confirmed by direct emissions of oxidation products methyl vinyl ketone and methacrolein. Global Change Biololgy **18:** 973–984

Jardine K, Sommer E, Saleska S, Huxman T, Harley P, Abrell L (2010) Gas Phase Measurements of Pyruvic Acid and Its Volatile Metabolites. Environmental Science & Technology **44:** 2454-2460

Jardine KJ, Meyers K, Abrell L, Alves EG, Serrano AM, Kesselmeier J, Karl T, Guenther A, Chambers JQ, Vickers C (2013) Emissions of putative isoprene oxidation products from mango branches under abiotic stress. Journal of Experimental Botany **64:** 3697-3709

Jardine KJ, Monson RK, Abrell L, Saleska SR, Arneth A, Jardine A, Ishida FY, Serrano AMY, Artaxo P, Karl T, Fares S, Goldstein A, Loreto F, Huxman T (2012b) Within-plant isoprene oxidation confirmed by direct emissions of oxidation products methyl vinyl ketone and methacrolein. Global Change Biology **18:** 973-984

Jones CA, Rasmussen RA (1975) Production of Isoprene by Leaf Tissue. Plant Physiology **55:** 982-987

Kameel FR, Riboni F, Hoffmann MR, Enami S, Colussi AJ (2014) Fenton Oxidation of Gaseous Isoprene on Aqueous Surfaces. The Journal of Physical Chemistry C

Karl T, Fall R, Rosenstiel T, Prazeller P, Larsen B, Seufert G, Lindinger W (2002a) On-line analysis of the $^{13}CO_2$ labelling of isoprene suggests multiple subcellular origins of isoprene precursors. Planta **215:** 894-905

Karl T, Fall R, Rosenstiel TN, Prazeller P, Larsen B, Seufert G, Lindinger W (2002b) On-line analysis of the (CO2)-C-13 labeling of leaf isoprene suggests multiple subcellular origins of isoprene precursors. Planta **215:** 894-905

Karl T, Harley P, Emmons L, Thornton B, Guenther A, Basu C, Turnipseed A, Jardine K (2010) Efficient atmospheric cleansing of oxidized organic trace gases by vegetation. Science **330:** 816-819

Kesselmeier J, Ciccioli P, Kuhn U, Stefani P, Biesenthal T, Rottenberger S, Wolf A, Vitullo M, Valentini R, Nobre A, Kabat P, Andreae MO (2002) Volatile organic compound emissions in relation to plant carbon fixation and the terrestrial carbon budget. Global Biogeochemical Cycles **16:** 1126-1135

Kimmerer TW, Macdonald RC (1987) Acetaldehyde and Ethanol Biosynthesis in Leaves of Plants. Plant Physiology **84:** 1204-1209

Laothawornkitkul J, Taylor JE, Paul ND, Hewitt CN (2009) Biogenic volatile organic compounds in the Earth system. New Phytologist **183:** 27-51

Laule O, Fürholz A, Chang H-S, Zhu T, Wang X, Heifetz PB, Gruissem W, Lange M (2003) Crosstalk between cytosolic and plastidial pathways of isoprenoid biosynthesis in Arabidopsis thaliana. Proceedings of the National Academy of Sciences **100:** 6866-6871

Lerdau M, Keller M (1997) Controls on isoprene emission from trees in a subtropical dry forest. Plant Cell and Environment **20:** 569-578

Lichtenthaler HK (2010) The Non-mevalonate DOXP/MEP (Deoxyxylulose 5-Phosphate/Methylerythritol 4-Phosphate) Pathway of Chloroplast Isoprenoid and Pigment Biosynthesis. *In* CA Rebeiz, C

Benning, HJ Bohnert, H Daniell, JK Hoober, HK Lichtenthaler, AR Portis, BC Tripathy, eds, The Chloroplast: Basics and Applications. Springer Netherlands, Dordrecht, 95-118

Loreto F, Delfine S (2000) Emission of isoprene from salt-stressed Eucalyptus globulus leaves. Plant Physiology **123:** 1605-1610

Loreto F, Mannozzi M, Maris C, Nascetti P, Ferranti F, Pasqualini S (2001) Ozone quenching properties of isoprene and its antioxidant role in leaves. Plant Physiololgy **126:** 993-1000

Loreto F, Pinelli P, Brancaleoni E, Ciccioli P (2004) ^{13}C labeling reveals chloroplastic and extrachloroplastic pools of dimethylallyl pyrophosphate and their contribution to isoprene formation. Plant Physiology **135:** 1903-1907

Loreto F, Schnitzler J-P (2010) Abiotic stresses and induced BVOCs. Trends in plant science **15:** 154-166

Loreto F, Sharkey TD (1990) A Gas-Exchange Study of Photosynthesis and Isoprene Emission in Quercus-Rubra L. Planta **182:** 523-531

Loreto F, Velikova V (2001) Isoprene produced by leaves protects the photosynthetic apparatus against ozone damage, quenches ozone products, and reduces lipid peroxidation of cellular membranes. Plant Physiology **127:** 1781-1787

Magel E, Mayrhofer S, Muller A, Zimmer I, Hampp R, Schnitzler JP (2006) Photosynthesis and substrate supply for isoprene biosynthesis in poplar leaves. Atmospheric Environment **40:** S138-S151

Monson RK, Fall R (1989) Isoprene Emission from Aspen Leaves - Influence of Environment and Relation to Photosynthesis and Photorespiration. Plant Physiology **90:** 267-274

Monson RK, Jaeger CH, Adams WW, Driggers EM, Silver GM, Fall R (1992) Relationships among Isoprene Emission Rate, Photosynthesis, and Isoprene Synthase Activity as Influenced by Temperature. Plant Physiology **98:** 1175-1180

Nguyen TB, Roach PJ, Laskin J, Laskin A, Nizkorodov SA (2011) Effect of humidity on the composition of isoprene photooxidation secondary organic aerosol. Atmospheric Chemistry and Physics **11:** 6931-6944

Pacifico F, Harrison SP, Jones CD, Sitch S (2009) Isoprene emissions and climate. Atmospheric Environment **43:** 6121-6135

Rasmussen R (1972) Survey of Plant Species That Release Isoprene to Atmosphere. Abstracts of Papers of the American Chemical Society

Rodríguez-Concepción M (2006) Early steps in isoprenoid biosynthesis: multilevel regulation of the supply of common precursors in plant cells. Phytochemistry Reviews **5:** 1-15

Rosenstiel TN, Potosnak MJ, Griffin KL, Fall R, Monson RK (2003) Increased CO_2 uncouples growth from isoprene emission in an agriforest ecosystem. Nature **421:** 256-259

Schnitzler J-P, Zimmer I, Bachl A, Arend M, Fromm J, Fischbach R (2005) Biochemical properties of isoprene synthase in poplar (Populus× canescens). Planta **222:** 777-786

Schnitzler JP, Graus M, Kreuzwieser J, Heizmann U, Rennenberg H, Wisthaler A, Hansel A (2004) Contribution of different carbon sources to isoprene biosynthesis in poplar leaves. Plant Physiology **135:** 152-160

Shah S, Rogers L (1969) Compartmentation of terpenoid biosynthesis in green plants. A proposed route of acetyl-coenzyme A synthesis in maize chloroplasts. Biochemical Journal **114:** 395-405

Sharkey TD, Loreto F (1993) Water-Stress, Temperature, and Light Effects on Isoprene Emission and Photosynthesis of Kudzu Leaves. Plant Physiology **102:** 159-159

Sharkey TD, Singsaas EL (1995) Why Plants Emit Isoprene. Nature **374:** 769-769

Silver GM, Fall R (1991) Enzymatic synthesis of isoprene from dimethylallyl diphosphate in aspen leaf extracts. Plant Physiology **97:** 1588-1591

Singsaas EL, Lerdau M, Winter K, Sharkey TD (1997) Isoprene increases thermotolerance of isoprene-emitting species. Plant Physiology **115:** 1413-1420

882 **Trowbridge AM, Asensio D, Eller ASD, Way DA, Wilkinson MJ, Schnitzler JP, Jackson RB, Monson RK**
883 (2012) Contribution of Various Carbon Sources Toward Isoprene Biosynthesis in Poplar Leaves
884 Mediated by Altered Atmospheric CO_2 Concentrations. Plos One **7**
885 **Vartapetian BB, Jackson MB** (1997) Plant adaptations to anaerobic stress. Annals of Botany **79:** 3-20
886 **Vartapetian BB, Pulli S, Fagerstedt K** (1997) Plant response and adaptation to anaerobiosis. Annals of
887 Botany **79**
888 **Velikova V, Sharkey T, Loreto F** (2012) Stabilization of thylakoid membranes in isoprene-emitting plants
889 reduces formation of reactive oxygen species. Plant Signal Behavior **7:** 139-141
890 **Velikova V, Varkonyi Z, Szabo M, Maslenkova L, Nogues I, Kovacs L, Peeva V, Busheva M, Garab G,**
891 **Sharkey TD, Loreto F** (2011) Increased Thermostability of Thylakoid Membranes in Isoprene-
892 Emitting Leaves Probed with Three Biophysical Techniques. Plant Physiology **157:** 905-916
893 **Vickers CE, Bongers M, Liu Q, Delatte T, Bouwmeester H** (2014) Metabolic engineering of volatile
894 isoprenoids in plants and microbes. Plant, Cell & Environment **37**: 1753-1775
895 **Vickers CE, Gershenzon J, Lerdau MT, Loreto F** (2009a) A unified mechanism of action for volatile
896 isoprenoids in plant abiotic stress. Nature Chemical Biology. **5:** 283-291
897 **Vickers CE, Possell M, Cojocariu CI, Velikova VB, Laothawornkitkul J, Ryan A, Mullineaux PM, Hewitt**
898 **CN** (2009b) Isoprene synthesis protects transgenic tobacco plants from oxidative stress. Plant
899 Cell & Environment **32:** 520-531
900 **Vickers CE, Possell M, Hewitt CN, Mullineaux PM** (2010) Genetic structure and regulation of isoprene
901 synthase in Poplar (Populus spp.). Plant Molecular Biology **73:** 547-558
902 **Vickers CE, Possell M, Laothawornkitkul J, Ryan AC, Hewitt CN, Mullineaux PM** (2011) Isoprene
903 synthesis in plants: lessons from a transgenic tobacco model. Plant Cell & Environment **34:** 1043-
904 1053
905 **Wildermuth MC, Fall R** (1996) Light-dependent isoprene emission (characterization of a thylakoid-
906 bound isoprene synthase in Salix discolor chloroplasts). Plant Physiology **112:** 171-182
907 **Wingler A, Quick W, Bungard R, Bailey K, Lea P, Leegood R** (1999) The role of photorespiration during
908 drought stress: an analysis utilizing barley mutants with reduced activities of photorespiratory
909 enzymes. Plant, Cell & Environment **22:** 361-373
910 **Zeidler J, Lichtenthaler F, May H** (1997) Is isoprene emitted by plants synthesized via the novel
911 isopentenyl pyrophosphate pathway? Zeitschrift für Naturforschung. C. A Journal of Biosciences
912 **52:** 15-23
913
914

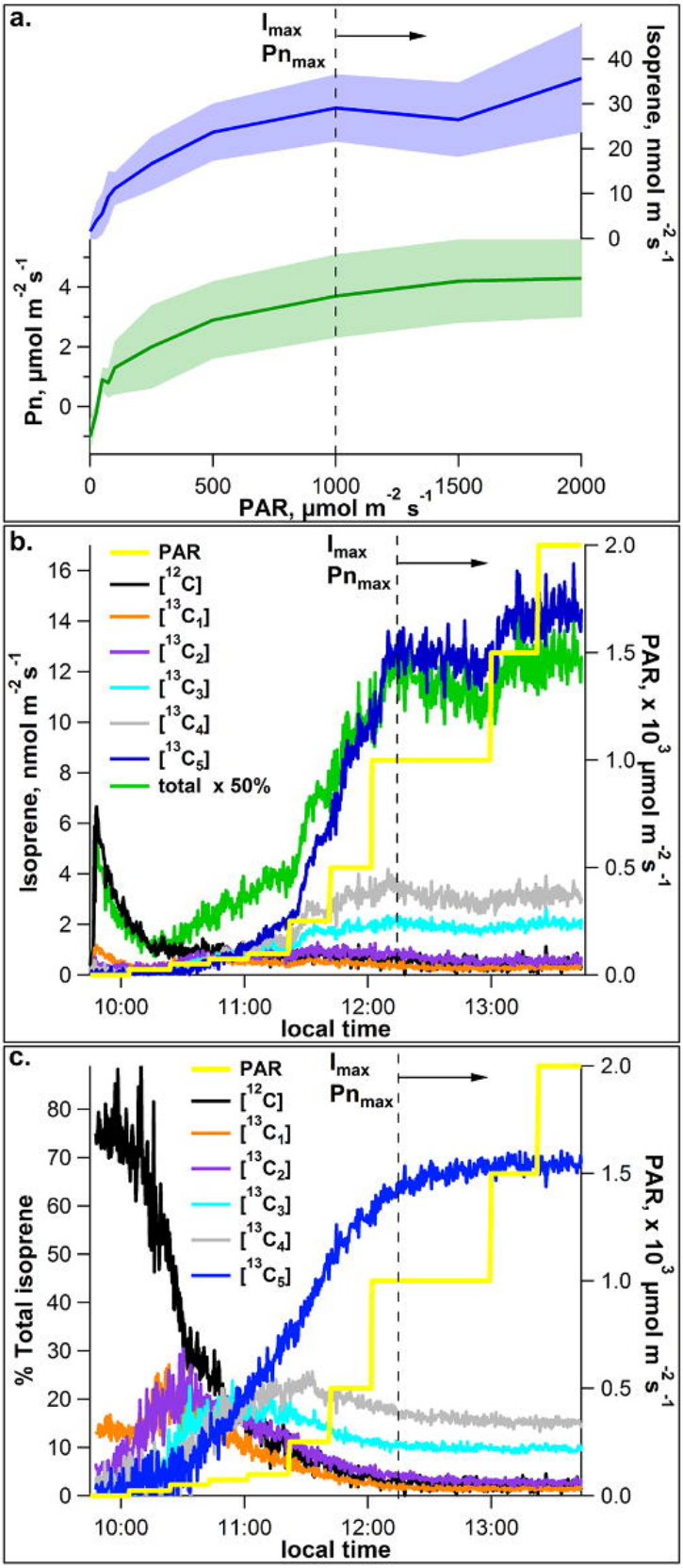

Figure 1: Dependencies of net photosynthesis (Pn) and isoprene emission rates from mango leaves on PAR intensities at a constant leaf temperature (30 °C). a) Average of leaf isoprene emissions (GC-MS; blue) and net photosynthesis rates (green) as a function of PAR from four mango leaves. Shaded areas represent +/- one standard deviation. Also shown are representative PTR-MS time series plots showing the influence of increasing PAR intensity on the dynamics of b) absolute emissions and c) relative emissions (% of total) of [^{12}C]isoprene and [$^{13}C_{1-5}$]isoprene from a single mango leaf during photosynthesis under $^{13}CO_2$. Vertical dashed lines represent optimum temperatures for net photosynthesis (Pn_{max}) and isoprene emissions (I_{max}).

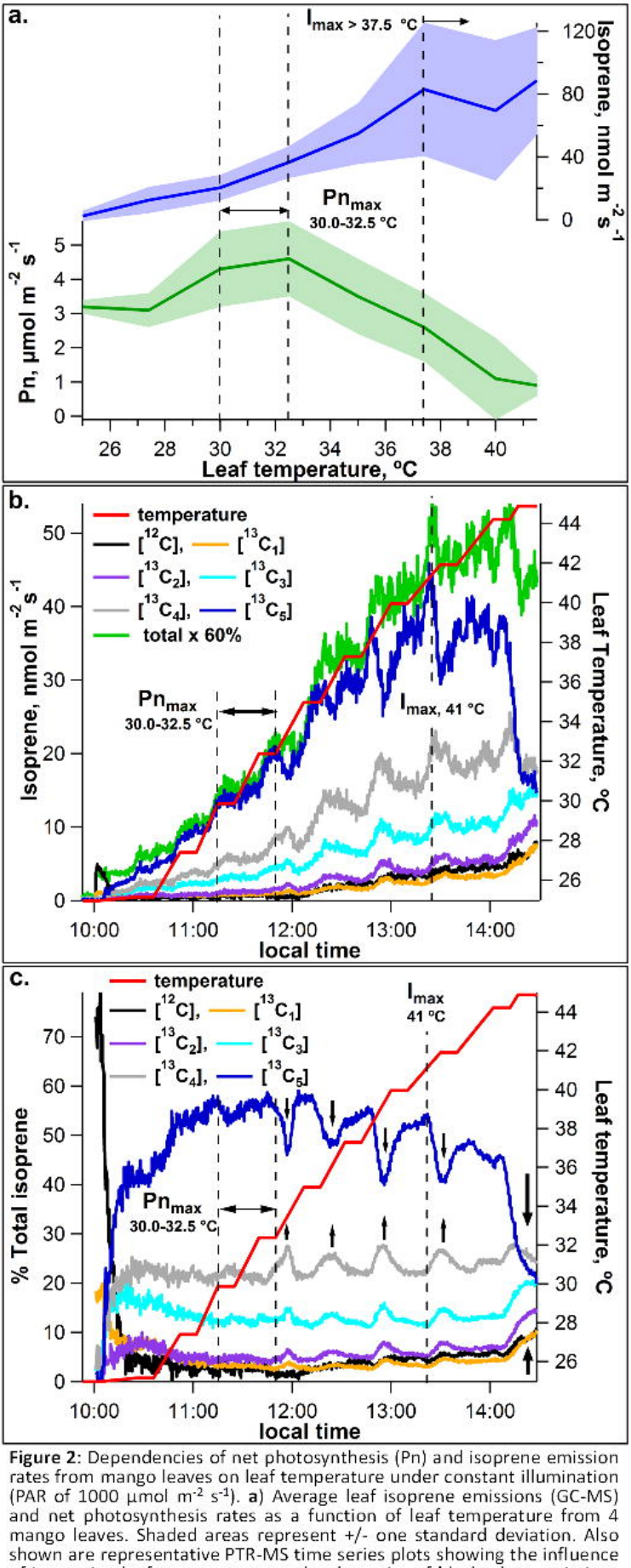

Figure 2: Dependencies of net photosynthesis (Pn) and isoprene emission rates from mango leaves on leaf temperature under constant illumination (PAR of 1000 µmol m^{-2} s^{-1}). **a**) Average leaf isoprene emissions (GC-MS) and net photosynthesis rates as a function of leaf temperature from 4 mango leaves. Shaded areas represent +/- one standard deviation. Also shown are representative PTR-MS time series plots showing the influence of increasing leaf temperature on the dynamics of **b**) absolute emissions of [^{12}C]isoprene and [$^{13}C_{1-5}$]isoprene and **c**) relative isoprene isotopologue emissions rates (% of total) from a single mango leaf during photosynthesis under $^{13}CO_2$. Arrows indicate periods of rapid of ^{13}C-depletion of isoprenoid intermediates followed by re-enrichment. Vertical dashed lines represent optimum temperature ranges for net photosynthesis (Pn_{max}) and isoprene emissions (I_{max}).

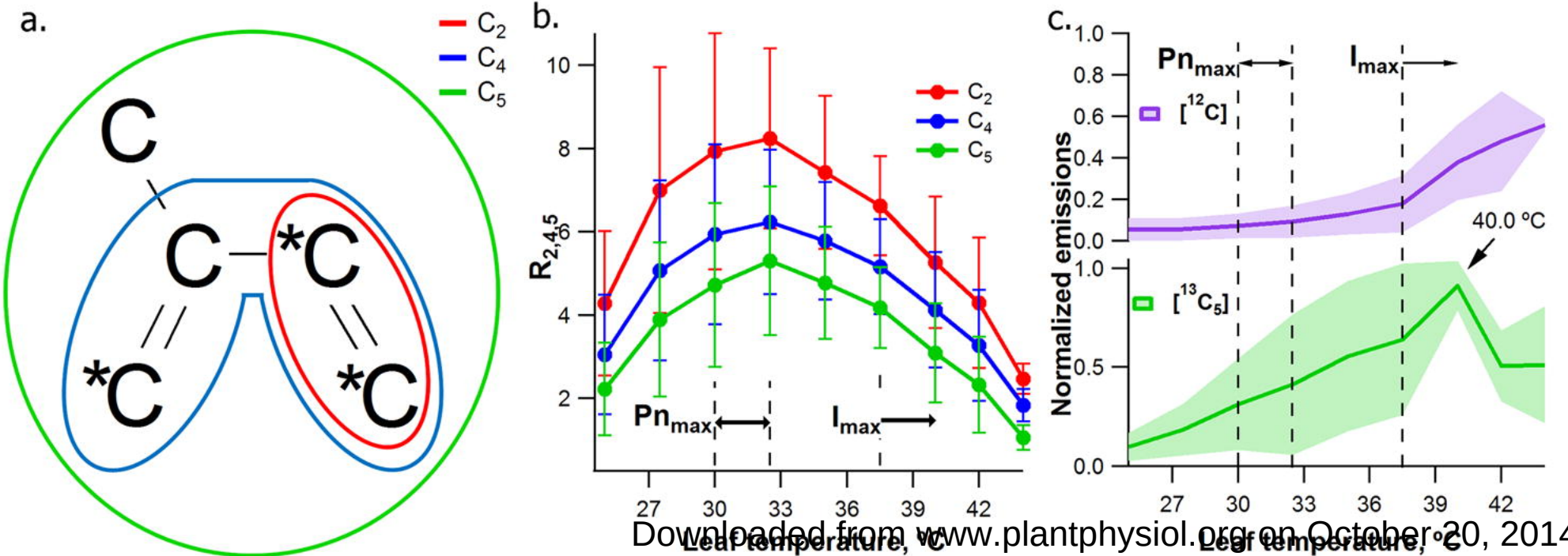

Figure 3: GC-MS ^{13}C-labeling analysis of isoprene emissions from 4 mango leaves during photosynthesis under $^{12}CO_2$ as a function of leaf temperature. **a**) Structure of isoprene GC-MS fragment ions with two carbon atoms (C_2, red) and four carbon atoms (C_4, blue) together with the isoprene parent ion with five carbon atoms (C_5, green). Carbon atoms derived from glyceraldehyde-3-phosphate (GA3P) and pyruvate are shown as *C and C respectively. **b**) Average $^{13}C/^{12}C$ isoprene emission ratios (R) of C_2 ($^{13}C_2/^{12}C_2$, R_2 = m/z 29/27) and C_4 ($^{13}C_4/^{12}C_4$, R_4 = m/z 57/53) fragment ions and C_5 ($^{13}C_5/^{12}C_5$, R_5 = m/z 73/68) parent ions. **c**) Average emission rates for [^{12}C]isoprene (m/z 68) and [$^{13}C_5$]isoprene (m/z 73) normalized to the maximum emissions of [$^{13}C_5$]isoprene. Vertical dashed lines represent optimum temperature ranges for net photosynthesis (Pn_{max}) and isoprene emissions (I_{max}).

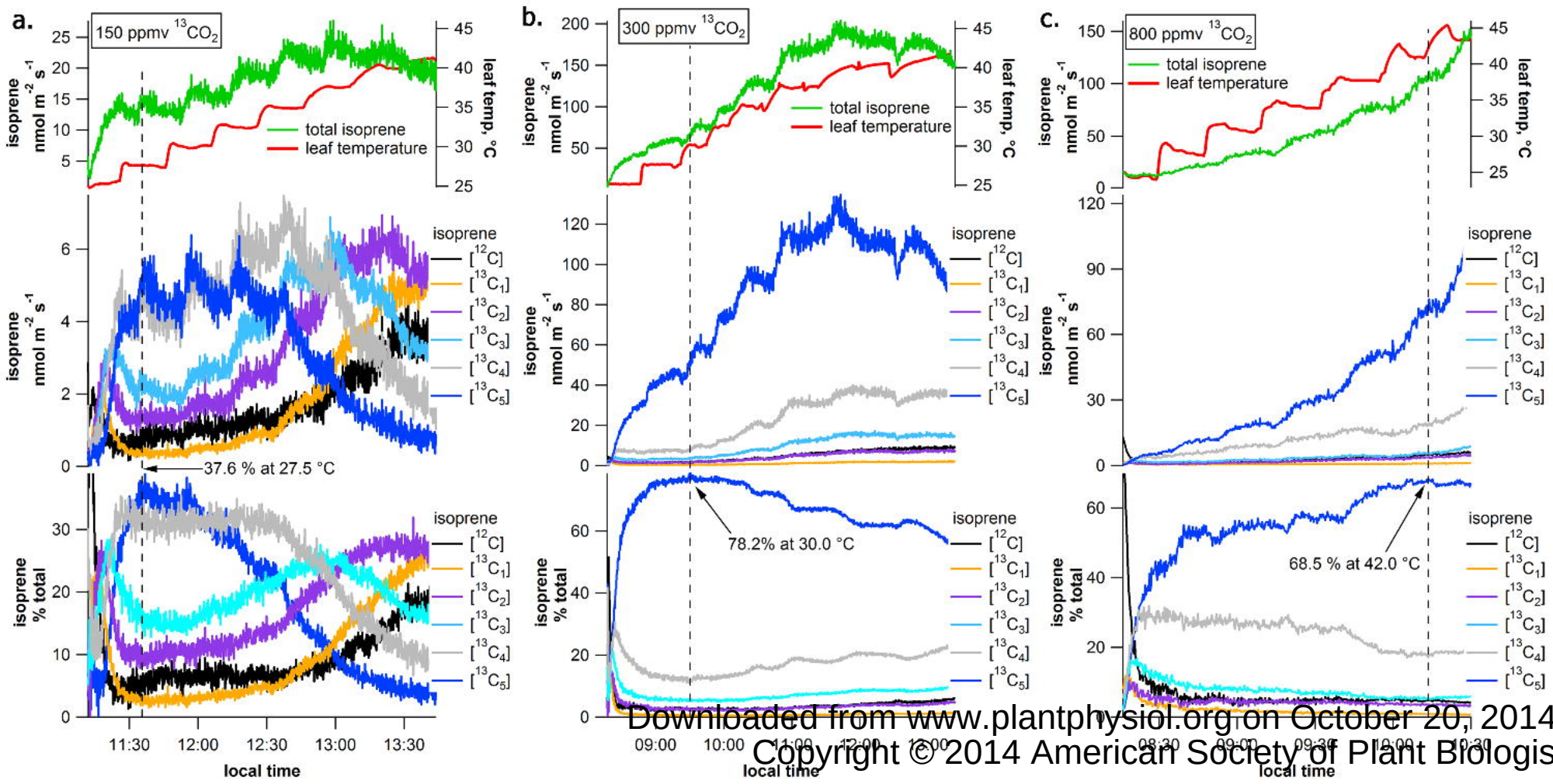

Figure 4: Representative PTR-MS time series plots showing absolute and relative emissions (% of total) of [^{12}C]isoprene and [$^{13}C_{1-5}$]isoprene as a function leaf temperature from three separate shimbillo leaves exposed to (**a**) 150, (**b**) 300, and (**c**) 800 ppm $^{13}CO_2$. Note that increased $^{13}CO_2$ concentrations strongly enhance the temperature corresponding to the maximum relative emissions of [$^{13}C_5$]isoprene (150 ppm: 27.5 °C, 300 ppm: 30.0 °C, 800 ppm: 42.0 °C).

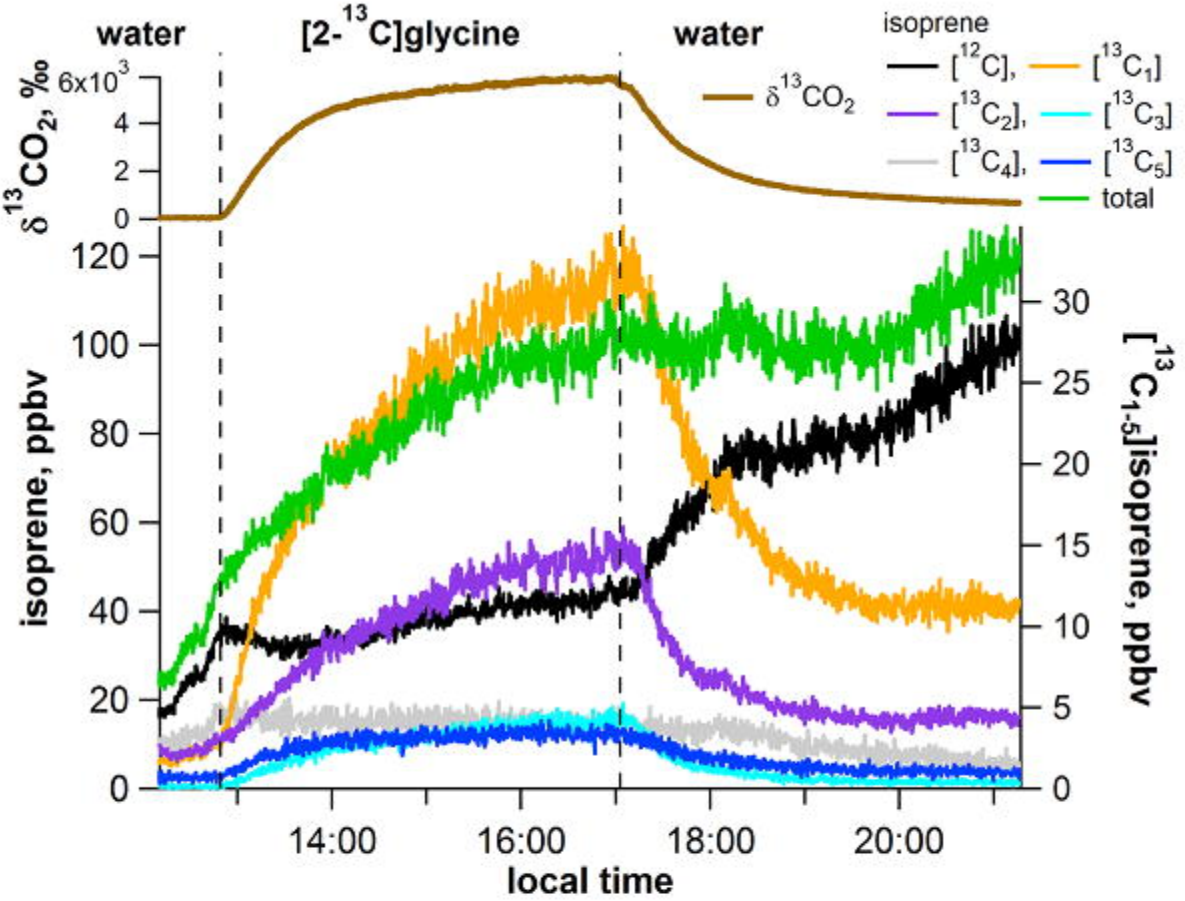

Figure 5: Representative CRDS and PTR-MS time series plot showing ^{13}C-labeling of photorespiratory CO_2 and isoprene during 10 mM [2-^{13}C]glycine feeding of a detached shimbillo branch through the transpiration stream under constant light (300-500 µmol m^{-2} s^{-1} PAR) and air temperature (28-30 °C). The detached branch was first placed in water, then transfered to the [2-^{13}C]glycine solution for four hours, before being replaced in water.

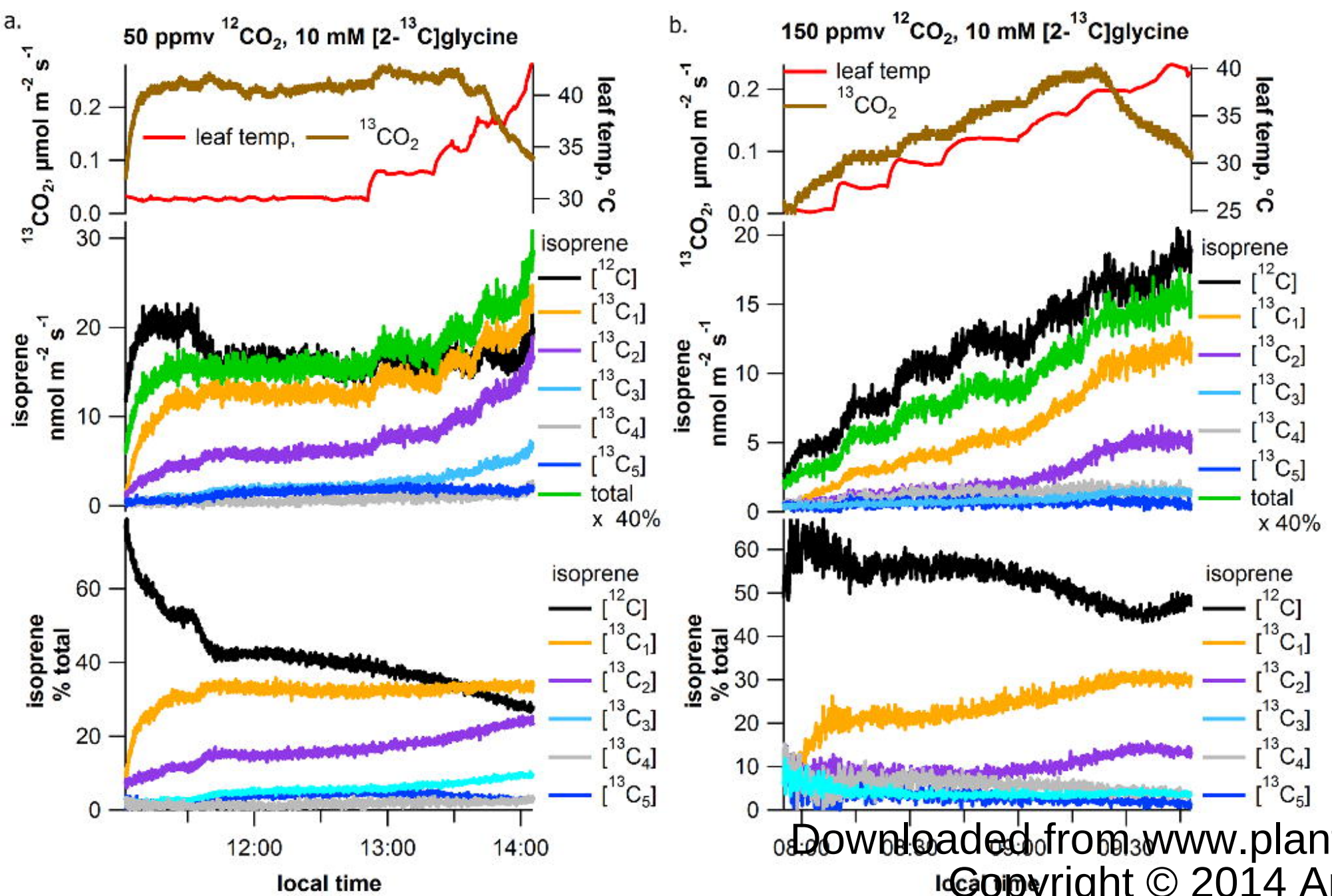

Figure 6: Representative CRDS and PTR-MS time series plots showing the influence of increasing leaf temperature on absolute emissions of photorespiratory $^{13}CO_2$, [^{12}C]isoprene and [$^{13}C_{1-5}$]isoprene from detached shimbillo leaves in a 10 mM [2-^{13}C]glycine solution under (a) 50 ppm $^{12}CO_2$ and (b) 150 ppm $^{12}CO_2$. Also shown are the relative emissions (% of total) of [^{12}C]isoprene and [$^{13}C_{1-5}$]isoprene. Note the general pattern of increasing relative emissions of [$^{13}C_{1-4}$]isoprene and a decrease in [^{12}C]isoprene with temperature.

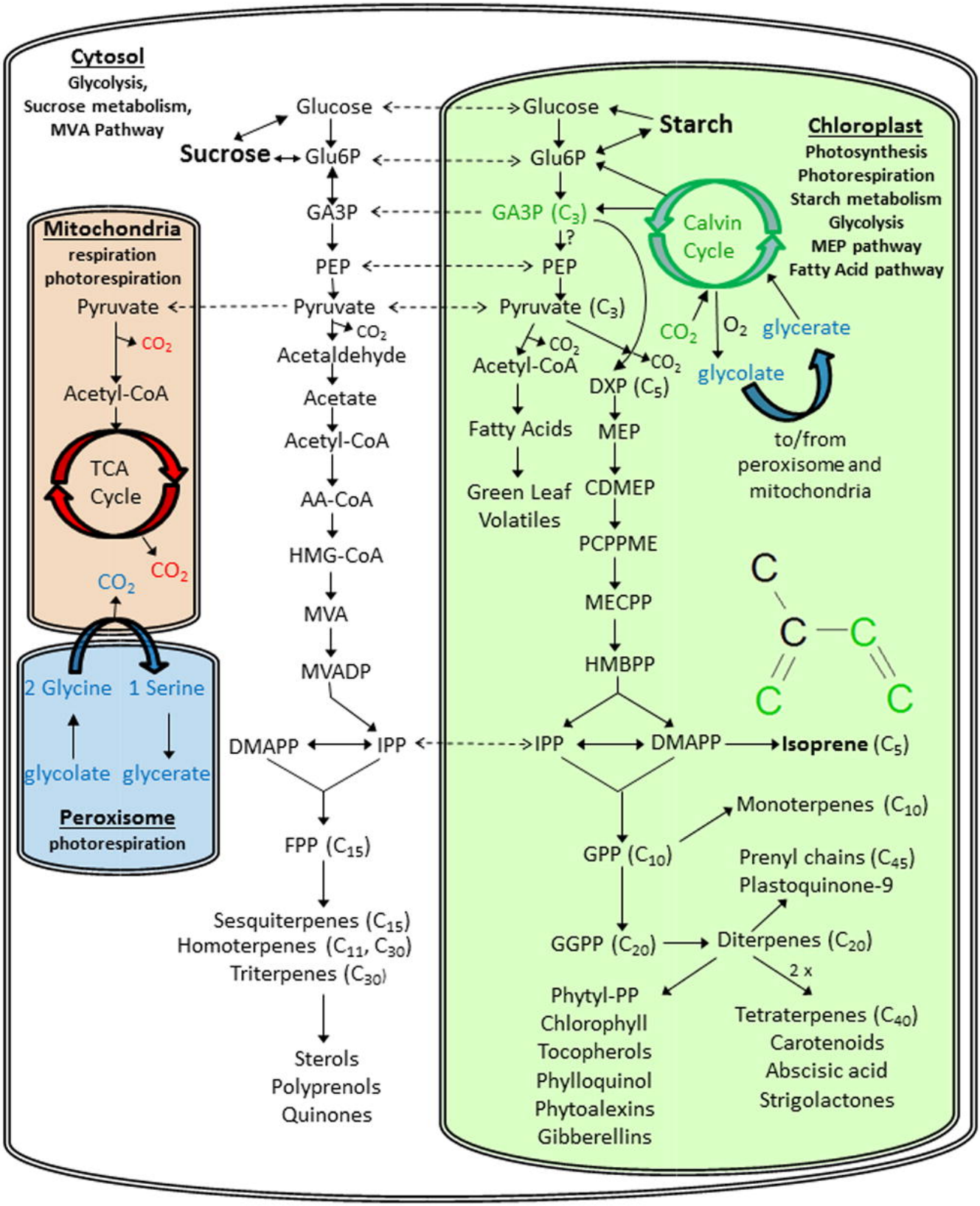

Figure 7: Simplified schematic of isoprenoid metabolism in photosynthetic plant cells and its relationship to photosynthesis, glycolysis, respiration, and photorespiration. Although the mevalonate (MVA) pathway is found in the cytosol and the methylerythritol phosphate (MEP) pathway is found in the chloroplast, some cross-talk occurs between the pathways through the exchange of intermediates (dashed arrows). CO_2 assimilated by the Calvin Cycle, entering the MEP pathway as GA3P, and ending up as carbon atoms 1-3 of isoprene are shown in green. Metabolite abbreviations include: Acetyl-CoA: acetyl-coenzyme A, AA-CoA: acetoacetyl-coenzyme A, CTP: cytidine 5′ triphosphate, CDMEP: 4-(cytidine 5′-diphospho)-2-C-methyl-D-erythritol, CMP: cytidine 5′-monophosphate, DMAPP: dimethylallyl pyrophosphate, DXP: 1-deoxy-D-xylulose-5-phosphate, FPP: farncyl pyrophosphate, GA3P: D-glyceraldehyde 3-phosphate, GPP: geranyl pyrophosphate, GGPP: geranyl geranyl pyrophosphate, G6P: glucose-6-phosphate, HMBPP: 1-hydroxy-2-methyl-2-(E)-butenyl 4-diphosphate, HMG-CoA: (S)-3-hydroxy-3-methylglutaryl-coenzyme A, IPP: isopentenyl pyrophosphate, MECPP: 2-C-methyl-D-erythritol-2,4-cyclodiphosphate, MEP: 2-C-methyl-D-erythritol-4-phosphate, MVA: (R)-mevalonate, MVAP: mevalonate-5-phosphate, MVADP: mevalonate diphosphate, PEP: phospho*enol*pyruvate, PCPPME: 2-phospho-4-(cytidine 5′-diphospho)-2-C-methyl-D-erythritol, Phytyl-PP: phytyl pyrophosphate. Figure modified from Vickers et al., 2009a and Vickers et al., 2014.